



UNIVERSITÀ DEL PIEMONTE ORIENTALE

SCHOOL OF MEDICINE

Department of Translational Medicine

PhD Program in Sciences and Medical Biotechnology

XXXII CYCLE

**BIOLOGICAL AND CLINICAL IMPLICATIONS
OF *BIRC3* MUTATIONS
IN CHRONIC LYMPHOCYTIC LEUKEMIA**

Tutor:

Chiar.mo Prof. Gianluca Gaidano

Coordinator:

Prof.ssa Marisa Gariglio

Candidate: Dr Chiara Favini

Matricula: 20022483

Accademic year 2018/2019

INDEX

SUMMARY	3
SOMMARIO	4
1. INTRODUCTION	5
2. AIM OF THE STUDY	7
3. MATERIALS AND METHODS	8
3.1. Patients.....	8
3.2. Cancer personalized profiling by deep sequencing (CAPP-seq).....	8
3.3. Bioinformatic pipeline for variant calling after CAPP-seq.....	9
3.4. Statistical analysis.....	11
3.5. Cell studies	12
3.6. Western blot analysis	12
3.7. RNA extraction and gene expression profiling.....	13
3.8. Knockdown of MAP3K14 by RNA interference	13
3.9. Inhibitor studies	14
3.10. <i>In vitro</i> drug responses in primary CLL cells	14
3.11. Apoptosis assay	15
4. RESULTS	16
4.1 Patients harboring <i>BIRC3</i> mutations are at risk of failing FCR	16
4.2 <i>BIRC3</i> mutations associate with activation of non-canonical NF- κ B signaling.....	17
4.3 <i>BIRC3</i> mutations confer resistance to fludarabine in primary CLL cells.....	19
5. DISCUSSION	20
6. REFERENCES.....	22
7. TABLES	28
8. FIGURES LEGENDS.....	30
8. FIGURES.....	33
9. SUPPLEMENTARY TABLES.....	39

SUMMARY

The current shift of therapy of chronic lymphocytic leukemia (CLL) towards novel targeted agents mandates the identification of molecular predictors to inform on who can still benefit from chemoimmunotherapy and who can be instead early considered for novel targeted agents. Fludarabine, cyclophosphamide, and rituximab (FCR) is the most effective chemoimmunotherapy regimen for the management of CLL and represents the current standard of care for young and fit patients devoid of *TP53* disruption. A retrospective multicenter cohort of 287 untreated patients receiving first-line FCR was analyzed by targeted next generation sequencing of 24 recurrently mutated genes in CLL. By univariate analysis adjusted for multiple comparisons *BIRC3* mutations identify a poor prognostic subgroup of patients failing FCR (median progression free survival: 2.2 years, $p < 0.001$) similar to cases harboring *TP53* mutations (median progression free survival: 2.6 years, $p < 0.0001$). *BIRC3* mutations maintained an independent association with an increased risk of progression with a hazard ratio of 2.8 (95% confidence interval 1.4-5.6, $p = 0.004$) in multivariate analysis adjusted for *TP53* mutation, 17p deletion and IGHV mutation status. The functional implications of *BIRC3* mutations are largely unexplored and little is known about the prognostic impact of *BIRC3* mutations in CLL cohorts homogeneously treated with first line FCR. By immunoblotting analysis, we showed that the non-canonical NF- κ B pathway is active in *BIRC3* mutated cell lines and in primary CLL samples, as documented by the stabilization of MAP3K14 and by the nuclear localization of p52. In addition, *BIRC3* mutated primary CLL cells are less sensitive to fludarabine. If validated, *BIRC3* mutations may be used as a new molecular predictor to select high-risk patients for novel frontline therapeutic approaches.

SOMMARIO

Le terapie innovative per la leucemia linfatica cronica (CLL) includono nuovi agenti i quali richiedono l'identificazione di predittori molecolari per determinare i pazienti che possono ancora beneficiare della chemio-immunoterapia e coloro che, invece, necessitano di trattamento con nuovi farmaci. La terapia di prima linea per pazienti giovani, in buone condizioni cliniche e privi di aberrazioni del gene *TP53*, prevede l'utilizzo dello schema immunochemioterapico FCR, la combinazione dei farmaci Fludarabina, Ciclofosfamide e Rituximab. Il DNA genomico di 287 pazienti, trattati con terapia secondo lo schema FCR, è stato raccolto alla diagnosi e sottoposto al sequenziamento di 24 geni ricorrentemente mutati nella CLL, mediante tecnica di Next Generation Sequencing (NGS). In analisi univariata, le mutazioni di *BIRC3* identificano un sottogruppo di pazienti con prognosi sfavorevole (sopravvivenza mediana libera da progressione: 2,2 anni, $p < 0,001$) simile ai casi che presentano mutazioni di *TP53* (sopravvivenza mediana libera da progressione: 2,6 anni, $p < 0,0001$). Le mutazioni di *BIRC3* rimangono associate ad un maggior rischio di progressione (HR) in analisi multivariata corretta per mutazione di *TP53*, delezione 17p e stato mutazionale di IGHV: HR 2,8 (95% I.C. 1,4-5,6, $p = 0,004$). Le implicazioni funzionali delle mutazioni di *BIRC3* sono in gran parte inesplorate e poco si conosce circa il loro impatto prognostico in coorti di pazienti trattati omogeneamente con FCR. Mediante analisi di immunoblotting è stato dimostrato che la via non canonica di NF- κ B è attiva sia nelle linee cellulari *BIRC3* mutate che nelle cellule primarie, come documentato dalla stabilizzazione di MAP3K14 e dalla localizzazione nucleare di p52. Inoltre, le cellule primarie *BIRC3* mutate sono meno sensibili al trattamento con Fludarabina. Se validate, le mutazioni di *BIRC3* potrebbero essere utilizzate come nuovo predittore molecolare per selezionare pazienti ad alto rischio per nuovi approcci terapeutici in prima linea.

1. INTRODUCTION

Chronic lymphocytic leukemia (CLL) is the most common type of adult leukemia in the western world with marked genetic and clinical variability.¹ The clinical course of CLL ranges from a very indolent condition, with a nearly normal life expectancy, to rapidly progressive leading to early death.² Fludarabine, cyclophosphamide, and rituximab (FCR) is the most effective chemoimmunotherapy regimen for the management of CLL, and represents the current standard for untreated patients who are young and in good physical condition^{3,4} except for patients with *TP53* alterations.⁵ Though the majority of CLL patients receiving FCR as frontline therapy are destined to relapse, a subgroup of cases may experience a durable first remission. The current shift of therapy of CLL towards novel targeted agents mandates the recognition of molecular predictors to identify patients who can still benefit from chemoimmunotherapy and those who should instead be considered for novel targeted agents upfront. In the case of FCR, the immunoglobulin heavy chain genes (IGHV) mutational status and Fluorescence In Situ Hybridization (FISH) karyotype stratify: *i*) low-risk patients carrying mutated IGHV genes and devoid of both del11q and del17p who maximally benefit from such treatment; *ii*) intermediate-risk patients harboring unmutated IGHV genes and/or del11q in the absence of del17p who are a case mix of good and poor responders to FCR; *iii*) high-risk patients harboring del17p who are unsuitable for chemoimmunotherapy.³ Deletion of 17p and *TP53* mutations capture most, routinely analyzed in clinical practice, but not all patients who are refractory to chemo-immunotherapy, which prompts the identification of additional biomarkers associated with early failure of FCR.³⁻⁵ B-cell neoplasia often pirates signaling pathways by molecular lesions to promote survival and proliferation. Though according to bioinformatics criteria *BIRC3* (also known as cIAP2) is one of the candidate driver genes of CLL, the functional implications of *BIRC3* mutations are partially unexplored.⁷⁻⁹

Nuclear factor- κ B (NF- κ B) signaling is a key component CLL development and evolution.¹⁰ Two NF- κ B pathways exist namely, canonical and noncanonical.¹¹ The former is triggered by the B-cell receptor (BCR) signaling via the Bruton's tyrosine kinase (BTK), while the latter is activated by members of the tumor necrosis factor (TNF) cytokine family.¹² Upon receptor binding, the TRAF3/MAP3K14-TRAF2/BIRC3 negative regulatory complex of non-canonical NF- κ B signaling is disrupted, MAP3K14 (also known as NIK), the central activating kinase of the pathway, is released and activated to induce the phosphorylation and proteasomal processing of p100, thereby leading to the formation of p52-containing NF- κ B dimers. The p52 protein dimerizes with RelB to translocate into the nucleus, where it regulates gene transcription. BIRC3 is a negative regulator of non-canonical NF- κ B. Physiologically, BIRC3 catalyzes MAP3K14 protein ubiquitination in a manner that is dependent on the E3 ubiquitin ligase activity of its C-terminal RING domain. MAP3K14 ubiquitination results into its proteasomal degradation.¹³ Also, little is known about the prognostic impact of *BIRC3* mutations in CLL cohorts homogeneously treated with first line FCR.

2. AIM OF THE STUDY

We aimed at refining the genetic-based stratification of FCR-treated CLL patients.

The aims of this study are:

- To identify molecular predictors in FCR treated patients;
- To assess the biological features underlying chemo-refractoriness to FCR.

3. MATERIALS AND METHODS

3.1. Patients

The study was designed as a retrospective observational analysis from a multicenter cohort of 287 (275 with complete clinical and molecular data) untreated CLL receiving first-line therapy with FCR in 17 different hematological centers. The following biological material was collected: *i*) 280 tumor genomic DNA (gDNA) and 7 tumor RNA isolated from peripheral blood (PB) before treatment start; and *ii*) paired germline gDNA from saliva from 14 cases. Normal gDNA from 22 healthy donors was also used to set the experimental background of the deep next generation sequencing (NGS) approach. Tumor and normal gDNA was extracted according to standard procedures.¹⁴ Tumor RNA was extracted according to the TRIzol Reagent protocol (Life Technologies). The clinical database was updated in April 2018. Patients provided informed consent in accordance with local Institutional Review Board requirements and the Declaration of Helsinki. The study was approved by the Ethical Committee of the Ospedale Maggiore della Carità di Novara associated with the Amedeo Avogadro University of Eastern Piedmont (study number CE 67/14).

3.2. Cancer personalized profiling by deep sequencing (CAPP-seq)

A targeted resequencing gene panel¹⁵ was designed to include: *i*) coding exons plus splice site of 24 CLL genes known to be implicated in CLL pathogenesis and/or prognosis; *ii*) 3'UTR of *NOTCH1*; and *iii*) enhancer and promoter region of *PAX5* (size of the target region: 66627bp) (Table S1).^{8,9} Tumor and germline gDNA were quantified using the Quant-iT™ PicoGreen dsDNA Assay kit (ThermoFisher Scientific) and 400 ng were sheared through sonication (Covaris M220 focused-ultrasonicator) before library construction to obtain 200-bp fragments. The size of the DNA fragments was checked using the Bioanalyzer

(Agilent Technologies). The NGS libraries for gDNA were constructed using the KAPA Library Preparation Kit (Kapa Biosystems) and NGS libraries for RNA were constructed using RNA Hyper Kit (Roche) following the manufacturer's instructions. Hybrid selection was performed with the custom SeqCap EZ Choice Library (Roche NimbleGen). Multiplexed libraries (n = 10 per run) were sequenced using 300-bp paired-end runs on a MiSeq sequencer (Illumina) to obtain a coverage of at least 2000x in >90% of the target region (66627bp) in 80% of cases (Table S2).

3.3. Bioinformatic pipeline for variant calling after CAPP-seq

Initially, FASTQ sequencing reads were deduped. We deduped FASTQ sequencing reads from gDNA by utilizing the FastUniq v1.1 software, that collapses as duplicate reads only those fragments (read pairs) with 100% sequence identity that also share genomic coordinates. The same approach was also used to dedupe germline gDNA and normal gDNA from 22 healthy donors, to avoid the introduction of biases in variant calling due to the application of different deduplication protocols. Then, the deduped FASTQ sequencing reads were locally aligned to the hg19 version of the human genome assembly using the BWA v.0.6.2 software with the default setting, and sorted, indexed and assembled into a mpileup file using SAMtools v.1. The aligned read families were processed with mpileup using the parameters -A -d 10000000. For cases provided with paired germline gDNA, single nucleotide variations and indels were called in tumor gDNA vs germline gDNA, respectively, with the somatic function of VarScan2 using the parameters min-coverage 1 --min-coverage-normal 1 --min-coverage-tumor 1 --min-var-freq 0--min-freq-for-hom 0.75 --somatic-p-value 0.05 --min-avg-qual 20 --strand-filter 1 --validation 1. For cases lacking paired germline gDNA, single nucleotide variations and indels were called in tumor gDNA using the CNS function of VarScan2 using the

parameters --min-coverage 0 --min-readedge 2 --min-avg-qual 20 --min-var-freq 0 --min-freq-for-hom 0.75 --p-value 0.05 --strand-filter 1 --output-vcf 1 --variants 0. The variants called by VarScan 2 were annotated using the SeattleSeq Annotation 138 tool by using the default setting. Variants annotated as SNPs according to dbSNP 138 (with the exception of *TP53* variants that were manually curated and scored as SNPs according to the IARC TP53 database), intronic variants mapping > 2 bp before the start or after the end of coding exons, and synonymous variants were then filtered out. The following strict post-processing filters were then applied to the remaining variants to further improve variant call confidence. To filter out variants below the base-pair resolution background frequencies in gDNA across the selector, for cases provided with paired germline gDNA, the Fisher's exact test was used to test whether the frequency of the variant called by VarScan 2 was significantly higher from that called in the corresponding paired germline gDNA, after adjusting for multiple comparisons by Bonferroni test [multiple comparisons corrected p threshold = 0.00000018761163, corresponding to alpha of 0.05/(66627 x 4 alleles per position)]. Accordingly, variants represented in > 10 reads of the paired germline and/or variants with a somatic p value from VarScan2 > 0.00000018761163 were no further considered. To filter out systemic sequencing errors, a database containing all germline and normal gDNA background allele frequencies was assembled. Based on the assumption that all background allele fractions follow a normal distribution, for both cases provided with paired germline gDNA and cases lacking paired gDNA, a Z-test was employed to test whether a given variant in the tumor gDNA differed significantly in its frequency from typical germline or normal gDNA background at the same position in all the other germline and normal gDNA samples, after adjusting for multiple comparisons by Bonferroni test [multiple comparisons corrected p threshold = 0.00000018761163, corresponding to alpha of 0.05/(66627 x 4 alleles per position)]. Variants that did not pass this filter were no

further considered. Variant allele frequencies for the resulting candidate mutations and the background error rate were visualized using IGV.

3.4. Statistical analysis

Progression free survival (PFS) was the primary endpoint and was measured from date of treatment start to date of progression according to IWCLL-NCI guidelines (event), death (event) or last follow-up (censoring). Overall survival (OS) was measured from date of initial presentation to date of death from any cause (event) or last follow-up (censoring). Survival analysis was performed by Kaplan-Meier method and compared between strata using the Log-rank test. A false discovery rate approach was used to account for multiple testing, and adjusted p-values were calculated using the Bonferroni correction. A maximally selected rank statistic was used to determine the optimal cut-off for variant allele frequency (VAF) based on the Log-rank statistics. A cut-off of 3% of VAF was set for *TP53* mutations and of 10% for all the other genes. The adjusted association between exposure variables and PFS was estimated by Cox regression. Internal validation of the multivariate analysis was performed using a bootstrap approach to estimate means and confidence intervals of hazard ratios (HR), and percentage of selection for each variable in the model. The number of bootstrap samples used was 1000. Statistical significance was defined as p value < 0.05. The analysis was performed with the Statistical Package for the Social Sciences (SPSS) software v.24.0 (Chicago, IL), with R statistical package 3.1.2 and with GraphPad version 7 (GraphPad Software Inc).

3.5. Cell studies

The human CLL cell line MEC1, the SMZL cell lines SSK41, VL51, and the MCL cell lines MAVER-1, Z-138 and JEKO-1 were cultured under standard conditions in RPMI-1640 medium with L-glutamine supplemented with 10% fetal calf serum (FCS), Penicillin (100 U/ml) and Streptomycin (100 U/ml) (Sigma Aldrich). Human HEK-293T cells were maintained in Iscove's Modified Dulbecco Medium (IMDM) supplemented with 10% fetal calf serum, 100 U/ml penicillin, 100 U/ml streptomycin and 2mM L-glutamine (Sigma Aldrich) under identical conditions.

Three primary cells samples known to harbor heterozygous inactivating mutations of *BIRC3* were included in the experiments. Two *BIRC3* wild type cases were used as controls.

3.6. Western blot analysis

The entire non-canonical NF- κ B pathway was assessed using the following specific primary antibodies: anti-BIRC3 (Cell Signaling, #3130), anti-TRAF2 (Cell Signaling, #4712), anti-TRAF3 (Cell Signaling, #4729), anti-MAP3K14 (Cell Signaling, #4994), anti-Phospho-NF- κ B2 p100 (Cell Signaling, #4810), anti-NF- κ B2 p100/p52 (Cell Signaling, #4882). Anti- β -actin (Sigma Aldrich, #A2066) was used as loading control. The Qproteome Nuclear Protein Kit (Qiagen) was used according to the manufacturer's instructions to isolate nuclear proteins from cells. Anti- β -tubulin (Sigma Aldrich, #T5201) and anti-BRG1 (G-7) (Santa Cruz Biotechnology, #17796) were used as controls for the purity of the cytoplasmic and nuclear fractions, respectively. Horseradish peroxidase-conjugated goat anti-mouse (LI-COR, #926-80010) or anti-rabbit (LI-COR, #926-80011) antibodies were used to highlight binding by enhanced chemiluminescence with the

Clarity Western ECL Substrate (Biorad). Image acquisition and densitometric analyses were performed using the Molecular Imager Gel Doc XR System and the Quantity One software (Biorad).

3.7. RNA extraction and gene expression profiling

Total RNA was extracted from exponentially growing cell lines by TRIzol reagent (Life Technologies), and retro-transcribed using the Reverse Transcription Kit (Applied Biosystems). Quantitative real-time PCR (qRT-PCR) was conducted with the Step One Plus apparatus (Step One software 2.0; Applied Biosystems) using commercially available TaqMan Gene expression assays (*TNFAIP3*: Hs00234713_m1; *NFKB2*: Hs00174517_m1; *NFKBIA*: Hs00153283_m1; *NFKBIE*: Hs00234431_m1; *PLEK*: Hs00950975_m1; *WNT10*: Hs00228741_m1; *IL2RG*: Hs00953624_m1; *RELB*: Hs00232389_m1; *MALT1*: Hs01120052_m1) (*BIRC3*: Hs00985031_g1) (Life Technologies). Reactions were done in triplicate from the same cDNA (technical replicates). The comparative CT method ($\Delta\Delta CT$) was used to calculate relative expression levels of the gene under analysis, using GAPDH (Hs03929097_g1) as internal references.

3.8. Knockdown of MAP3K14 by RNA interference

Lentiviruses expressing 3 short hairpin RNAs (shRNAs) targeting MAP3K14, as well as the scrambled shRNA, were produced and cloned into the BamHI/HindIII cloning sites of the pGFP-C-shLenti vectors (OriGene Technologies). Within the 5'-LTR and 3'-LTR regions, each pGFP-C-shLenti vector contains an shRNA expression cassette driven by an U6 promoter, a puromycin resistance marker driven by a SV40 promoter and a GFP driven by a CMV promoter. The shRNA expression cassette consists of 29 bp target-gene-specific sequence, a 7 bp loop, and another 29 bp reverse complementary sequence, followed by a

TTTTTT termination sequence. The HEK293T cell line was co-transfected with expression (3 different pGFP-C-MAP3K14-shLenti or pGFP-C-non-effective-shLenti) vectors and adjuvant vectors (pMDL, REV and VSV-G). Fluorescence microscope was utilized to check the expression of the GFP in the transfected HEK293T cell line. After virus titration, the VL51 cell line was infected with lentiviruses harboring the shRNAs against MAP3K14 and the scrambled through a spinoculation protocol. After four days, infected cells were monitored by flow cytometry for the expression of the GFP and were selected by puromycin (1.5 µg/mL). Cell viability was monitored by Tripan blue counting.

3.9. Inhibitor studies

Cells were put under starvation in RPMI 0.1% Fetal Bovine Serum (FBS) 24h before treatment. Then they were seeded at 8000 cells per well in a 96-well U-bottom plate and treated with 1 µM, 5 µM and 10 µM of Ibrutinib (PCI-32765, Selleckchem) or vehicle (DMSO). Relative growth was determined by a Cell-Titer Glo (CTG) Luminescent Cell Viability Assay (Promega) 72h and 96h after treatment, according to the manufacturer's instructions and luminescence was quantified using a Victor X (PerkinElmer) multilabel reader. Treatments were done in triplicate (biological replicates).

3.10. *In vitro* drug responses in primary CLL cells

Leukemic cells were purified using Ficoll-Hypaque (Sigma Aldrich) from PB of CLL patients. Staining with CD19 and CD5 confirmed that in all samples leukemic cells were >90%. Patients were then divided into *BIRC3* mutated (MUT) or wild-type (WT). *TP53* mutated samples (and *BIRC3* WT) were selected as positive control (i.e., cells intrinsically resistant to therapies). Cells were cultured in RPMI 10% FCS (200 µl, all

reagents from Sigma) at a density of 5×10^6 /ml and both dose- and time-dependent responses were analyzed. Specifically, CLL cells were exposed to fludarabine) for 24-48 hours. Fludarabine was used at 1-5-10-25 μ M and venetoclax at 5-10-50-100-500-2000 nM.

3.11. Apoptosis assay

Drug-induced apoptosis was measured using the eBioscience™ Annexin V Apoptosis Detection Kit APC (ThermoFisher) following the manufacturer's instruction. Data were acquired using a FACSCanto II cytofluorimeter (BD Biosciences) and processed with DIVA v6.1.3 and FlowJo Version 9.01 (TreeStar). Apoptosis assays were analyzed using the two-way ANOVA test.

4. RESULTS

4.1 Patients harboring *BIRC3* mutations are at risk of failing FCR

Mutational profiling was performed in 287 patients who received first line FCR. The baseline features of the study cohort were consistent with progressive, previously untreated CLL (Table 1). The median follow-up was 6.8 years, with a median PFS and OS of 4.6 and 11.7 years, respectively (Table 1) consistent with clinical trial cohorts.¹⁶ As expected, *SF3B1* and *NOTCH1* were the most frequently mutated genes identified in 13.9% and in 13.6% of patients respectively, followed by *TP53* in 9.4% and *ATM* in 6.9% of patients, reflecting the data reported in previous studies.^{8,9,17} Overall, 154/287 (53.6%) cases harbored at least one non-synonymous somatic mutation in one of the 24 CLL genes included in our panel (range: 1-5 mutation per patient), which is consistent with the typical mutational spectrum of the coding genome of CLL requiring first line treatment. (Figure 1; Table S3).^{8,9,18} Outside of the coding genome, we identified one single mutation in the 3' region of *NOTCH1* (c.*378A>G) already reported.⁸

By univariate analysis adjusted for multiple comparisons, among the genes analyzed in our panel, only *TP53* mutations (median PFS of 2.6 years; $p < 0.0001$) and *BIRC3* mutations (median PFS of 2.2 years; $p < 0.001$) (Figure 2 A) associated with significantly shorter PFS (Table 2). The PFS after FCR of *BIRC3* mutated patients was similar to that of cases harboring *TP53* disruption (Figure 2 B). Consistently, *BIRC3* mutated patients had a lower likelihood of achieving complete response (22.2%) at the end of FCR compared to *BIRC3* wild type cases (76.7%; $p=0.001$). Well known molecular prognostic biomarkers of CLL, such as unmutated IGHV gene status and 17p deletion also associated with a significantly shorter PFS, supporting the representativeness of the study cohort (Table 2). By multivariate analysis including variables showing a

multiplicity adjusted significant association with PFS, *BIRC3* mutations maintained an independent association with PFS, with a HR of 2.8 (95% C.I. 1.4-5.6, $p = 0.004$) (Table 2).

4.2 *BIRC3* mutations associate with activation of non-canonical NF- κ B signaling

In order to comprehensively map unique *BIRC3* mutations in CLL, we compiled somatically confirmed variants identified in the current CLL study cohort with those identified in previous studies¹⁷ or listed in public CLL mutation catalogues (Figure 3 A). Virtually all *BIRC3* mutations were represented by frameshift or stop codons clustering in two hotspot regions comprised between amino acid 367-438 and amino acid 537-564. *BIRC3* variants were predicted to generate aberrant truncated transcripts causing the elimination or truncation of the C-terminal RING domain of the BIRC3 protein. The RING domain of BIRC3 harbors the E3 ubiquitin ligase activity that is essential for proteasomal degradation of MAP3K14, the central activating kinase of the noncanonical NF- κ B signaling. This observation points to non-canonical NF- κ B activation through MAP3K14 stabilization as the predicted functional consequence of *BIRC3* mutations in CLL. The non-canonical NF- κ B signaling was profiled by immunoblotting in B-cell tumor cell lines and primary CLL cells with different genetic make-up in the non-canonical NF- κ B pathway to verify whether *BIRC3* mutations lead to constitutive non-canonical NF- κ B activation. Additional genetic features of the above mentioned cell lines and primary CLL cells are shown in Table S4. In the VL51 SMZL cell line and in the MEC1 CLL cell lines, both harboring endogenous truncating mutations of the *BIRC3* gene, non-canonical NF- κ B signaling was constitutively active, as documented by the stabilization of MAP3K14, phosphorylation of NF- κ B₂, its processing from p100 to p52, as well as nuclear localization of p52 (Figure 3 B-D). Consistent with the biochemical clues of non-canonical NF- κ B activation, the gene expression signature of the VL51 and MEC1

cell lines was significantly enriched of non-canonical NF- κ B target genes (Figure 3 E-F). Non-canonical NF- κ B signaling in *BIRC3* mutated cells was consistent with that of MCL cell lines known to harbor a disrupted TRAF3/MAP3K14-TRAF2/BIRC3 negative regulatory complex by loss of TRAF3 or TRAF2.¹⁹ As *BIRC3* mutated cell lines, also primary CLL samples harboring inactivating mutations of *BIRC3* showed stabilization of MAP3K14 and NF- κ B2 processing from p100 to p52 (Figure 3 C), thus confirming that non-canonical NF- κ B activation is also a feature of primary cells harboring *BIRC3* variants.

MAP3K14 was genetically targeted by shRNA to test whether *BIRC3* mutated cells are addicted of its stabilization. Compared to non-targeting shRNA, the most efficient anti MAP3K14 shRNA-D resulted in a partial silencing of MAP3K14 and in a decreased NF- κ B₂ processing from p100 to p52. This translated into a reduced cell viability of the *BIRC3* mutated VL51 cell line transduced with shRNA-D. This observation indicates that MAP3K14 stabilization is a vulnerability of *BIRC3* mutated cells (Figure 4).

In order to test the contribution of BTK to noncanonical NF- κ B signaling when it is activated through *BIRC3* mutations, *BIRC3* mutated cell lines, as well as cell lines harboring a disrupted or competent TRAF3/MAP3K14-TRAF2/BIRC3 negative regulatory complex were treated with ibrutinib at different dosage and non-canonical NF- κ B signaling activation probed by immunoblotting of the NF- κ B2 processing from p100 to p52. Processing from p100 to p52 was unaffected by ibrutinib treatment in cell lines harboring *BIRC3* mutations (Figure 5) or a disrupted TRAF3/MAP3K14-TRAF2/BIRC3 negative regulatory complex consistent with the notion that *BIRC3* mutations activate non-canonical NF- κ B by bypassing BTK blockade by ibrutinib¹⁹.

4.3 *BIRC3* mutations confer resistance to fludarabine in primary CLL cells

We performed *in vitro* pharmacological studies on primary CLL cells to verify the vulnerabilities of *BIRC3* mutated cells. CLL cells purified from patients carrying *BIRC3* mutations were treated with increasing doses of fludarabine. Drug-induced apoptosis was compared to samples harboring *TP53* mutations, which represent a control for fludarabine resistance. CLL cells devoid of genetic lesions on either *BIRC3* or *TP53* were adopted as a control cohort for fludarabine sensitivity. Molecular characteristic of the *ex-vivo* CLL cells are listed in Table S5. *BIRC3* mutated cells showed a delayed fludarabine-induced cell death, as no response was observed after 24-hour treatment, at variance with *TP53* and *BIRC3* wild type samples. At this time point, cell viability curves of *BIRC3* mutated samples were almost completely overlapping with that of *TP53* disrupted samples, which are known to be fludarabine resistant (Figure 6 A). At 48 hours, *BIRC3* mutated cells had viability that was lower than that of *TP53* mutated samples, but higher than that of *TP53* and *BIRC3* wild type samples (Figure 6 B).

In order to assess whether *BIRC3* mutations interfere with apoptosis, primary CLL cells were treated with venetoclax. Venetoclax treatment resulted in similar reduction of cell viability in *BIRC3* mutated cells, *TP53* mutated cells and *BIRC3/TP53* wild type cells (Figure 6 C, D). Such divergent sensitivity to fludarabine and venetoclax of *BIRC3* mutated CLL cells indirectly suggests that *BIRC3* mutations likely affect the upstream DNA damage response pathway rather than the downstream apoptosis among mechanisms of cell death induction.

5. DISCUSSION

The results of this study provide the evidence that: *i)* *BIRC3* mutated patients fail FCR chemoimmunotherapy analogous to cases harboring *TP53* disruption; and that *ii)* *BIRC3* mutations associate with activation of the non-canonical NF- κ B pathway and with resistance to fludarabine *in vitro*.

The mere presence of somatic mutations is insufficient to implicate a gene in cancer. Cancer geneticists and bioinformaticians differentiate “passengers” events, likely being randomly acquired, to distinguish them from mutations targeting candidate “cancer driver” genes, likely implicated in the tumor biology, according to a statistical definition. Any given gene is labeled as candidate “cancer driver” if it harbors somatic point mutations at a statistically significant rate or pattern in cancer samples. In CLL, more than 40 genes fulfill the statistical definition of candidate “cancer driver”, including *BIRC3*, but few of them are biologically validated (i.e. *SF3B1*, *NOTCH1*, *TP53*, *ATM*, *FBXW7*).^{8,9,20-23} The *BIRC3* (Baculoviral IAP Repeat Containing 3) gene codes for a protein that ubiquitinates and negatively regulates the central activating kinase of the non-canonical NF- κ B pathway, namely MAP3K14.^{24,25} In lymphoid malignancies, the NF- κ B pathway is a pivotal and positive mediator of cell proliferation and survival.^{7,26,27} In CLL, *BIRC3* mutations are absent in monoclonal B-cell lymphocytosis (MBL) patients, are rare at the time of diagnosis (3-4%), but are detectable in approximately 25% of fludarabine refractory patients.¹⁷ In this study, we verified the biological consequences of *BIRC3* mutations by showing that they associate with activation of the non-canonical NF- κ B pathway, that *BIRC3* mutated lymphoid cells are addicted of non-canonical NF- κ B pathway, and that *BIRC3* mutated CLL are resistant to fludarabine both *in vitro* and in patients. It still remains to be clarified whether NF- κ B activation is the only molecular pathway that causes chemo-refractoriness in *BIRC3* mutated CLL or whether other mechanisms are also involved.²⁷⁻³¹

The introduction of FCR has represented a breakthrough in the management of young and fit CLL patients with an improvement in both PFS and OS compared to previous regimens. In both clinical trials and real life cohorts,³⁻⁵ IGHV mutation status and *TP53* disruption sorted out as strong predictors of poor response to FCR. However, these molecular biomarkers do not fully capture all high-risk patients destined to relapse. We propose *BIRC3* mutations as a new biomarker for the identification of high-risk patients failing FCR similarly to cases harboring *TP53* disruption. If validated in independent series, *BIRC3* mutations may turn out as a new molecular predictor of FCR resistance to be use for selecting patients to be treated with novel targeted agents.

Non-canonical NF- κ B activation by *BIRC3* mutations by-pass the block of BTK by ibrutinib. Consistently, NF- κ B activation and cell survival is unaffected by ibrutinib in both CLL cells (our study) and mantle cell lymphoma cells.¹⁹ If this pre-clinical evidence will be validated in ibrutinib-treated patients, *BIRC3* mutations may translate in a biomarker also for informing selection of novel agents.

6. REFERENCES

1. Zhang S, Kipps TJ. The pathogenesis of chronic lymphocytic leukemia. *Annu Rev Pathol.* 2014;9:103-18.
2. Rossi D, Gaidano G. The clinical implications of gene mutations in chronic lymphocytic leukemia. *Br J Cancer.* 2016;114(8):849-54.
3. Rossi D, Terzi-di-Bergamo L, De Paoli L, Cerri M, Ghilardi G, Chiarenza A, Bulian P, Visco C, Mauro FR, Morabito F, Cortelezzi A, Zaja F, Forconi F, Laurenti L, Del Giudice I, Gentile M, Vincelli I, Motta M, Coscia M, Rigolin GM, Tedeschi A, Neri A, Marasca R, Perbellini O, Moreno C, Del Poeta G, Massaia M, Zinzani PL, Montillo M, Cuneo A, Gattei V, Foà R, Gaidano G. Molecular prediction of durable remission after first-line fludarabine-cyclophosphamide-rituximab in chronic lymphocytic leukemia. *Blood.* 2015;126(16):1921-4.
4. Fischer K, Bahlo J, Fink AM, Goede V, Herling CD, Cramer P, Langerbeins P, von Tresckow J, Engelke A, Maurer C, Kovacs G, Herling M, Tausch E, Kreuzer KA, Eichhorst B, Böttcher S, Seymour JF, Ghia P, Marlton P, Kneba M, Wendtner CM, Döhner H, Stilgenbauer S, Hallek M. Long-term remissions after FCR chemoimmunotherapy in previously untreated patients with CLL: updated results of the CLL8 trial. *Blood.* 2016;127(2):208-15.
5. Thompson PA, Tam CS, O'Brien SM, Wierda WG, Stingo F, Plunkett W, Smith SC, Kantarjian HM, Freireich EJ, Keating MJ. Fludarabine, cyclophosphamide, and rituximab treatment achieves long-term disease-free survival in IGHV-mutated chronic lymphocytic leukemia. *Blood.* 2016;127(3):303-9.

6. Hallek M, Cheson BD, Catovsky D, Caligaris-Cappio F, Dighiero G, Döhner H, Hillmen P, Keating M, Montserrat E, Chiorazzi N, Stilgenbauer S, Rai KR, Byrd JC, Eichhorst B, O'Brien S, Robak T, Seymour JF, Kipps TJ. Guidelines for diagnosis, indications for treatment, response assessment and supportive management of chronic lymphocytic leukemia. *Blood*. 2018;131(25):2745-2760.
7. Asslaber D, Wacht N, Leisch M, Qi Y, Maeding N, Hufnagl C, Jansko B, Zaborsky N, Villunger A, Hartmann TN, Greil R, Egle A. BIRC3 expression predicts CLL progression and defines treatment sensitivity via enhanced NF- κ B nuclear translocation. *Clin Cancer Res*. 2019;25(6):1901-1912.
8. Puente XS, Beà S, Valdés-Mas R, Villamor N, Gutiérrez-Abril J, Martín-Subero JI, Munar M, Rubio-Pérez C, Jares P, Aymerich M, Baumann T, Beekman R, Belver L, Carrio A, Castellano G, Clot G, Colado E, Colomer D, Costa D, Delgado J, Enjuanes A, Estivill X, Ferrando AA, Gelpí JL, González B, González S, González M, Gut M, Hernández-Rivas JM, López-Guerra M, Martín-García D, Navarro A, Nicolás P, Orozco M, Payer ÁR, Pinyol M, Pisano DG, Puente DA, Queirós AC, Quesada V, Romeo-Casabona CM, Royo C, Royo R, Rozman M, Russiñol N, Salaverría I, Stamatopoulos K, Stunnenberg HG, Tamborero D, Terol MJ, Valencia A, López-Bigas N, Torrents D, Gut I, López-Guillermo A, López-Otín C, Campo E. Non-coding recurrent mutations in chronic lymphocytic leukaemia. *Nature*. 2015;526(7574):519-524.
9. Landau DA, Tausch E, Taylor-Weiner AN, Stewart C, Reiter JG, Bahlo J, Kluth S, Bozic I, Lawrence M, Böttcher S, Carter SL, Cibulskis K, Mertens D, Sougnez CL, Rosenberg M, Hess JM, Edelmann J, Kless S, Kneba M, Ritgen M, Fink A, Fischer K, Gabriel S, Lander ES, Nowak MA, Döhner H, Hallek M, Neuberg D, Getz G, Stilgenbauer S, Wu CJ. Mutations driving CLL and their evolution in progression and relapse. *Nature*. 2015;526(7574):525-530.

10. Mansouri L, Papakonstantinou N, Ntoufa S, Stamatopoulos K, Rosenquist R. NF- κ B activation in chronic lymphocytic leukemia: A point of convergence of external triggers and intrinsic lesions. *Semin Cancer Biol.* 2016;39:40-48
11. Bonizzi G, Karin M. The two NF-kappaB activation pathways and their role in innate and adaptive immunity. *Trends Immunol.* 2004;25(6):280-288.
12. Oeckinghaus A, Hayden MS, Ghosh S. Crosstalk in NF- κ B signaling pathways. *Nat Immunol.* 2011;12(8):695-708.
13. Sun SC. The noncanonical NF- κ B pathway. *Immunol Rev.* 2012;246(1):125-140.
14. Miller SA, Dykes DD, Polesky HF. A simple salting out procedure for extracting DNA from human nucleated cells. *Nucleic Acids Res.* 1988;16(3):1215.
15. Newman AM, Bratman SV, To J, Wynne JF, Eclov NC, Modlin LA, Liu CL, Neal JW, Wakelee HA, Merritt RE, Shrager JB, Loo BW Jr, Alizadeh AA, Diehn M. An ultrasensitive method for quantitating circulating tumor DNA with broad patient coverage. *Nat Med.* 2014;20(5):548-554.
16. Hallek M, Fischer K, Fingerle-Rowson G, Fink AM, Busch R, Mayer J, Hensel M, Hopfinger G, Hess G, von Grünhagen U, Bergmann M, Catalano J, Zinzani PL, Caligaris-Cappio F, Seymour JF, Berrebi A, Jäger U, Cazin B, Trneny M, Westermann A, Wendtner CM, Eichhorst BF, Staib P, Bühler A, Winkler D, Zenz T, Böttcher S, Ritgen M, Mendila M, Kneba M, Döhner H, Stilgenbauer S; International Group of Investigators; German Chronic Lymphocytic Leukaemia Study Group. Addition of rituximab to fludarabine and cyclophosphamide in patients with chronic lymphocytic leukaemia: a randomised, open-label, phase 3 trial. *Lancet.* 2010;376(9747):1164-1174.

17. Rossi D, Fangazio M, Rasi S, Vaisitti T, Monti S, Cresta S, Chiaretti S, Del Giudice I, Fabbri G, Bruscatin A, Spina V, Deambrogi C, Marinelli M, Famà R, Greco M, Daniele G, Forconi F, Gattei V, Bertoni F, Deaglio S, Pasqualucci L, Guarini A, Dalla-Favera R, Foà R, Gaidano G. Disruption of BIRC3 associates with fludarabine chemorefractoriness in TP53 wild-type chronic lymphocytic leukemia. *Blood*. 2012;119(12):2854-2862.
18. Stilgenbauer S, Schnaiter A, Paschka P, Zenz T, Rossi M, Döhner K, Bühler A, Böttcher S, Ritgen M, Kneba M, Winkler D, Tausch E, Hoth P, Edelmann J, Mertens D, Bullinger L, Bergmann M, Kless S, Mack S, Jäger U, Patten N, Wu L, Wenger MK, Fingerle-Rowson G, Lichter P, Cazzola M, Wendtner CM, Fink AM, Fischer K, Busch R, Hallek M, Döhner H. Gene mutations and treatment outcome in chronic lymphocytic leukemia: results from the CLL8 trial. *Blood*. 2014;123(21):3247-3254.
19. Rahal R, Frick M, Romero R, Korn JM, Kridel R, Chan FC, Meissner B, Bhang HE, Ruddy D, Kauffmann A, Farsidjani A, Derti A, Rakiec D, Naylor T, Pfister E, Kovats S, Kim S, Dietze K, Dörken B, Steidl C, Tzankov A, Hummel M, Monahan J, Morrissey MP, Fritsch C, Sellers WR, Cooke VG, Gascoyne RD, Lenz G, Stegmeier F. Pharmacological and genomic profiling identifies NF-κB targeted treatment strategies for mantle cell lymphoma. *Nature Medicine*. 2014;20(1):87-92.
20. Grossmann V, Kohlmann A, Schnittger A, Weissmann S, Jeromin S, Kienast J, Kern W, Haferlach T, Haferlach C. Recurrent ATM and BIRC3 mutations in patients with chronic lymphocytic leukemia (CLL) and deletion 11q22-q23. *Blood*. 2012;120(21):1771.
21. Rose-Zerilli MJ, Forster J, Parker H, Parker A, Rodríguez AE, Chaplin T, Gardiner A, Steele AJ, Collins A, Young BD, Skowronska A, Catovsky D, Stankovic T, Oscier DG, Strefford JC. ATM mutation rather than

- BIRC3 deletion and/or mutation predicts reduced survival in 11q-deleted chronic lymphocytic leukemia: data from the UK LRF CLL4 trial. *Haematologica*. 2014;99(4):736-742.
22. Baliakas P, Hadzidimitriou A, Sutton LA, Rossi D, Minga E, Villamor N, Larrayoz M, Kminkova J, Agathangelidis A, Davis Z, Tausch E, Stalika E, Kantorova B, Mansouri L, Scarfò L, Cortese D, Navrkalova V, Rose-Zerilli MJ, Smedby KE, Juliusson G, Anagnostopoulos A, Makris AM, Navarro A, Delgado J, Oscier D, Belessi C, Stilgenbauer S, Ghia P, Pospisilova S, Gaidano G, Campo E, Strefford JC, Stamatopoulos K, Rosenquist R; European Research Initiative on CLL (ERIC). Recurrent mutations refine prognosis in chronic lymphocytic leukemia. *Leukemia*. 2015;29(2):329-336.
 23. Nadeu F, Delgado J, Royo C, Baumann T, Stankovic T, Pinyol M, Jares P, Navarro A, Martín-García D, Beà S, Salaverria I, Oldreive C, Aymerich M, Suárez-Cisneros H, Rozman M, Villamor N, Colomer D, López-Guillermo A, González M, Alcoceba M, Terol MJ, Colado E, Puente XS, López-Otín C, Enjuanes A, Campo E. Clinical impact of clonal and subclonal TP53, SF3B1, BIRC3, NOTCH1, and ATM mutations in chronic lymphocytic leukemia. *Blood*. 2016;127(17):2122-2130.
 24. Vince JE, Wong WW, Khan N, Feltham R, Chau D, Ahmed AU, Benetatos CA, Chunduru SK, Condon SM, McKinlay M, Brink R, Leverkus M, Tergaonkar V, Schneider P, Callus BA, Koentgen F, Vaux DL, Silke J. IAP antagonists target cIAP1 to induce TNF α -dependent apoptosis. *Cell*. 2007;131(4):682-693.
 25. Jost PJ, Ruland J. Aberrant NF-kappaB signaling in lymphoma: mechanisms, consequences, and therapeutic implications. *Blood*. 2007;109(7):2700-2707.
 26. Raponi S, Del Giudice I, Ilari C, Cafforio L, Messina M, Cappelli LV, Bonina S, Piciocchi A, Marinelli M, Peragine N, Mariglia P, Mauro FR, Rigolin GM, Rossi F, Bomben R, Dal Bo M, Del Poeta G, Diop F, Favini C, Rossi D, Gaidano G, Cuneo A, Gattei V, Guarini A, Foá R. Biallelic BIRC3 inactivation in chronic

lymphocytic leukaemia patients with 11q deletion identifies a subgroup with very aggressive disease.

Br J Haematol. 2019;185(1):156-159.

27. Hewamana S, Lin TT, Jenkins C, Burnett AK, Jordan CT, Fegan C, Brennan P, Rowntree C, Pepper C. The novel nuclear factor-kappaB inhibitor LC-1 is equipotent in poor prognostic subsets of chronic lymphocytic leukemia and shows strong synergy with fludarabine. *Clin Cancer Res.* 2008;14(24):8102-8111.
28. Beg AA, Baltimore D. An essential role for NF- κ B in preventing TNF- α -induced cell death. *Science.* 1996;274:782–784.
29. Wang CY, Mayo MW, Baldwin AS, Jr. TNF- and cancer therapy-induced apoptosis: potentiation by inhibition of NF- κ B. *Science.* 1996;274:784–787.
30. Webster GA, Perkins ND. Transcriptional cross talk between NF- κ B and p53. *Mol Cell Biol.* 1999;19:3485–3495.
31. Nakanishi C, Toi M. Nuclear factor- κ B inhibitors as sensitizers to anticancer drugs. *Nat Rev.* 2005;5:297–309

7. TABLES

Table 1. Clinical data of FCR-treated CLL patients

Characteristics	Number of patients (%)	Total
Male	198 (69.0%)	N=287
Female	89 (31.0%)	
Binet A	33 (11.5%)	N=287
Binet B-C	254 (88.5%)	
<i>IGHV</i> mutated	100 (35.7%)	N=280
<i>IGHV</i> unmutated	180 (64.3%)	
17p deletion	13 (4.7%)	N=274
No 17p deletion	261 (95.3%)	
11q deletion	47 (17.2%)	N=273
No 11q deletion	226 (82.8%)	
13q deletion	111 (40.7%)	N=273
No 13q deletion	162 (50.3%)	
Trisomy 12	50 (18.4%)	N=272
No Trisomy 12	222 (81.6%)	
Median Follow-up (years)	6.8	
Median PFS	4.6	
PFS % (7-years)	31.0%	
Median OS (years)	11.7	
OS % (7-years)	75.5%	

PFS, progression free survival; OS, overall survival; *IGHV*, immunoglobulin heavy variable gene.

Table 2. Univariate and multivariate analysis of PFS

Characteristics	Univariate analysis					Multivariate analysis				Internal bootstrapping validation			
	7-y PFS (%)	Median PFS (y)	95% CI	<i>P</i>	<i>P</i> *	HR	LCI	UCI	<i>P</i>	HR	LCI	UCI	Bootstrapping selection (%)
Binet A	40.3%	4.5	2.4-6.6	0.356	-	-	-	-	-	-	-	-	-
Binet B-C	30.0%	4.6	3.8-5.4			-	-	-		-	-	-	
<i>IGHV</i> mutated	49.3%	6.5	3.8-9.2	<0.001	0.003	-	-	-	0.001	-	-	-	98.8%
<i>IGHV</i> unmutated	23.0%	3.9	3.5-4.4			1.8	1.3	2.6		1.9	1.3	2.7	
No 11q deletion	33.4%	5.0	4.2-5.9	0.025	0.700	-	-	-	-	-	-	-	-
11q deletion	13.9%	3.6	2.4-4.9			-	-	-		-	-	-	
No 17p deletion	33.0%	4.8	4.1-5.6	<0.0001	<0.0001	-	-	-	<0.0001	-	-	-	99.5%
17p deletion	nr	1.1	0-2.6			4.0	2.2	7.5		4.9	2.5	9.8	
<i>TP53</i> Wild type	33.8%	5.4	4.3-5.8	<0.0001	<0.001	-	-	-	0.030	-	-	-	73.3%
<i>TP53</i> Mutated	nr	2.8	2.0-3.5			1.7	1.1	2.8		1.8	1.1	3	
<i>BIRC3</i> Wild type	32.2%	4.8	4.1-5.6	<0.001	0.005	-	-	-	0.004	-	-	-	91.1%
<i>BIRC3</i> Mutated	nr	2.2	0.9-3.5			2.8	1.4	5.6		3.4	1.6	7.3	
<i>EGR2</i> Wild type	31.5%	4.7	3.9-5.4	0.015	0.420	-	-	-	-	-	-	-	-
<i>EGR2</i> Mutated	nr	1.5	0-3.8			-	-	-		-	-	-	
<i>ATM</i> Wild type	32.5%	4.8	4.1-5.6	0.029	0.812	-	-	-	-	-	-	-	-
<i>ATM</i> Mutated	nr	3.2	2.4-4.1			-	-	-		-	-	-	

P, P-value; *P**, Bonferroni correction; PFS, progression free survival; CI, confidence interval; HR, hazard ratio; LCI, lower confidence interval; UCI, upper confidence interval; *IGHV*, immunoglobulin heavy variable gene; nr, not reached

8. FIGURES LEGENDS

Figure 1. Mutational profile of the FCR-treated cohort. Case-level mutational profiles of 287 patients FCR-treated patients. Each column represents one tumor sample, each row represents one gene. The fraction of tumors with mutations in each gene is plotted on the right. The number and type of mutations in each patient is plotted above the heat map. Mutations are highlighted in red. IGHV mutational status, 17p deletion and 11q deletion are plotted in the bottom of the heatmap.

Figure 2. Kaplan-Meier estimates of progression free survival in *BIRC3* mutated patients. (A) Cases harboring *BIRC3* mutations are represented by the red line. Cases wild type for this gene are represented by the blue line. **(B)** Cases harboring *BIRC3* mutations are represented by the red line. Cases harboring *TP53* disruption (including *TP53* mutation and/or 17p deletion) are represented by the yellow line. Patients devoid of *BIRC3* mutation and *TP53* disruption are represented by the blue line. The Log-rank statistics p values are indicated adjacent curves.

Figure 3: Non-canonical NF- κ B pathway is active in *BIRC3* mutated CLL cell lines and primary samples.

(A) Disposition of *BIRC3* mutations across the protein. The mutations identified by Landau et al.⁹, Puente et al.⁸ and from public CLL mutation catalogue (COSMIC v85) are plotted in grey. Individual *BIRC3* mutations identified in the current studied cohort and in our previous study¹⁷ are plotted in red. **(B)** Western blot analysis of *BIRC3* protein expression and NF- κ B₂ activation and processing in the SMZL cell lines SSK41, VL51 and in the CLL cell line MEC1, carrying wild-type or disrupted *BIRC3*. The MAVER-1 and

Z-138 cell lines were used as positive controls of non-canonical NF- κ B activation, harboring genetic activation of non-canonical NF- κ B signaling. The JEKO-1 and HEK 293T cell lines were used as negative controls for non-canonical NF- κ B signalling. α -actin was used as a loading control. Color codes indicate the gene status in each cell lines. The aberrant BIRC3 band expressed in MEC1 and VL51 cell lines correspond in size to the predicted BIRC3-truncated protein, encoded by the mutant allele. **(C)** Western blot analysis showing BIRC3 expression and NF- κ B2 processing in purified primary tumor cells from 5 CLL and SMZL patients carrying wild-type or disrupted BIRC3. Color codes indicate the gene status in each cell lines. The aberrant *BIRC3* bands in patients 09321, 14462 and 12603 correspond in size to the predicted BIRC3-truncated protein encoded by the mutant allele. α -actin was used as a loading control. **(D)** Western blot of whole cell extract, cytoplasmic or nuclear fractions of the SMZL and CLL cell lines probed for the NF- κ B₂ subunits p100 and p52. The MAVER-1 and Z-138 cell lines served as positive controls while the JEKO-1 and HEK 293T cell lines were used as negative controls. β -tubulin and BRG1 served as controls for the purity of the cytoplasmic and nuclear fractionations, respectively. **(E)** GSEA enrichment score and distribution of non-canonical NF- κ B target genes along the rank of transcripts differentially expressed in the SMZL cell lines SSK41, VL51 and in the CLL cell line MEC1. The JEKO-1 cell line was used as negative control. **(F)** Validation of non-canonical NF- κ B target genes expression in the same SMZL and CLL cell lines as determined by quantitative real-time RT-PCR. Changes of genes expression were normalized to GAPDH expression; relative quantities were log₂ normalized to control samples (MCL cell line JEKO-1).

Figure 4: Knockdown of MAP3K14 by RNA interference in VL51 cells. **(A)** Western blot analysis for MAP3K14 expression and for NF- κ B₂ processing of p100 to p52. **(B)** VL51 cells viability assessed by trypan

blue after transduction with lentiviral vectors expressing the shRNAD_MAP3K14 (in red), a scrambled shRNA (in blu), and in non transfected cells (in green).

Figure 5: Non-canonical NF- κ B pathway is not switched off by ibrutinib in *BIRC3* mutated cell lines.

Western blot showing p100/p52 expression in **(A)** MEC1 and **(B)** VL51 cell lines that harbors *BIRC3* mutations. **(C)** MAVER-1 and **(D)** Z-138 cell lines, known to be affected by noncanonical NF- κ B pathway gene mutations and resistant to ibrutinib were used as positive controls. **(E)** JEKO-1 cell line, known to be devoid of NF- κ B pathway gene mutations and sensitive to ibrutinib was used as negative control. All cell lines were treated with different concentrations of ibrutinib for 72 and 96 hours.

Figure 6: Responses of primary cells lines to fludarabine and venetoclax. Viability of *BIRC3* mutated (n = 6 patients, red line), *TP53* mutated (n = 8 patients, black line) and wild type (n = 7 patients, blue line) primary CLL cells treated with different concentrations of fludarabine for **(A)** 24 hours and **(B)** 48 hours and of venetoclax for **(C)** 24 hours and **(D)** 48 hours. The pairwise p values have been listed in the tables below the respective figures. M, mutated; WT, wild type; NT, not treated.

8. FIGURES

Figure 1. Mutational profile of the FCR-treated cohort.

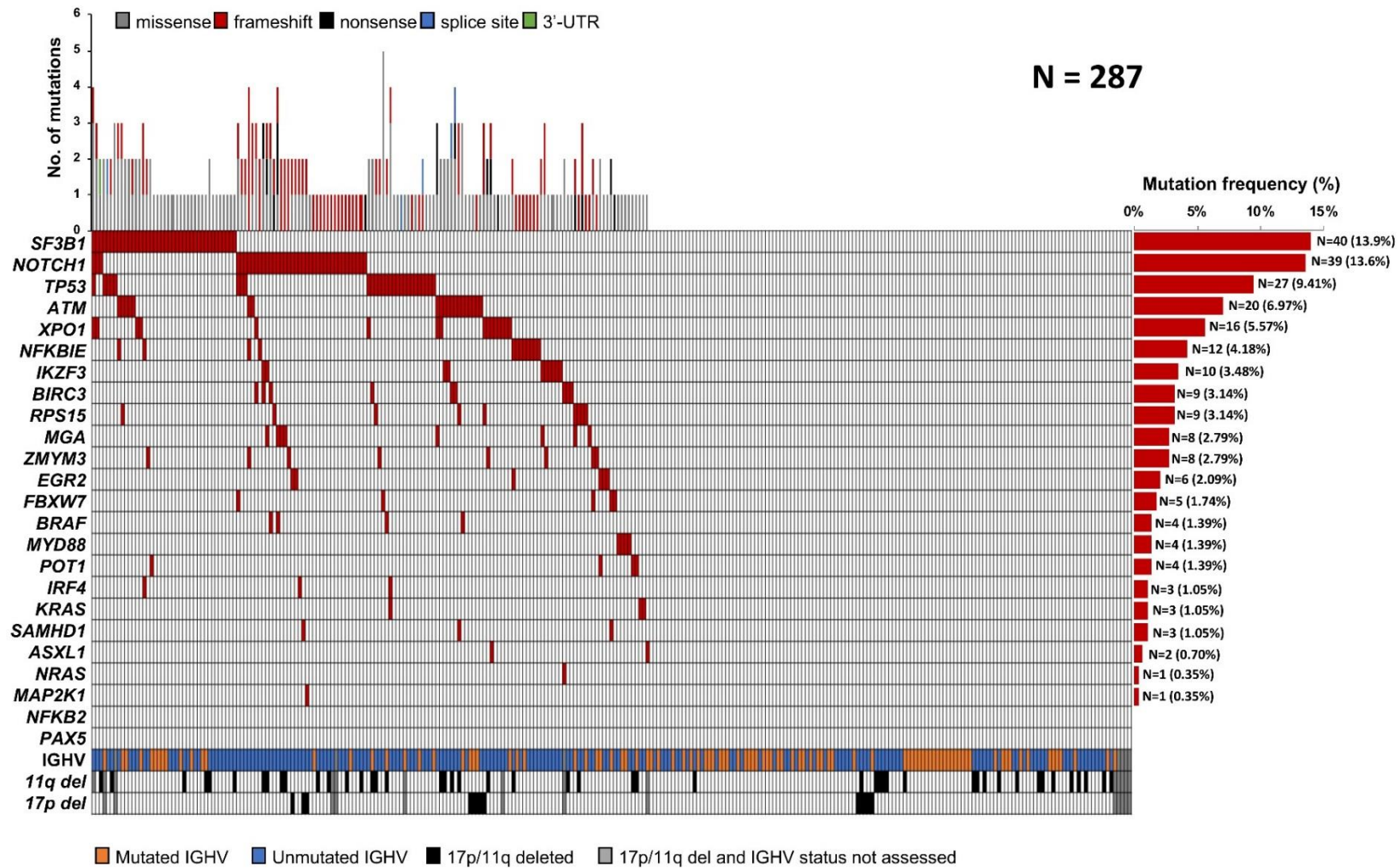


Figure 2. Kaplan-Meier estimates of progression free survival in *BIRC3* mutated patients.

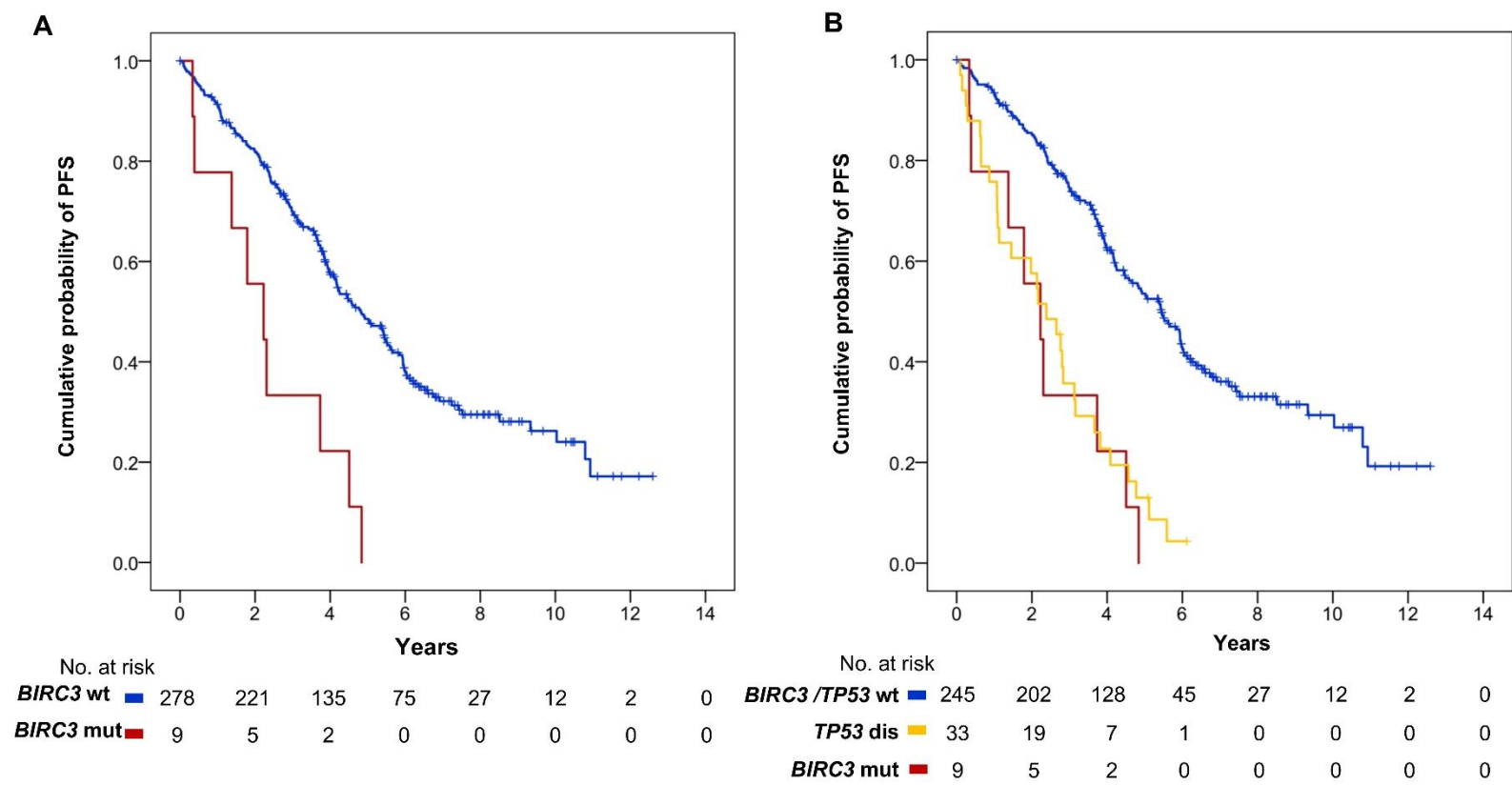


Figure 3: Non-canonical NF- κ B pathway is active in *BIRC3* mutated CLL cell lines and primary samples.

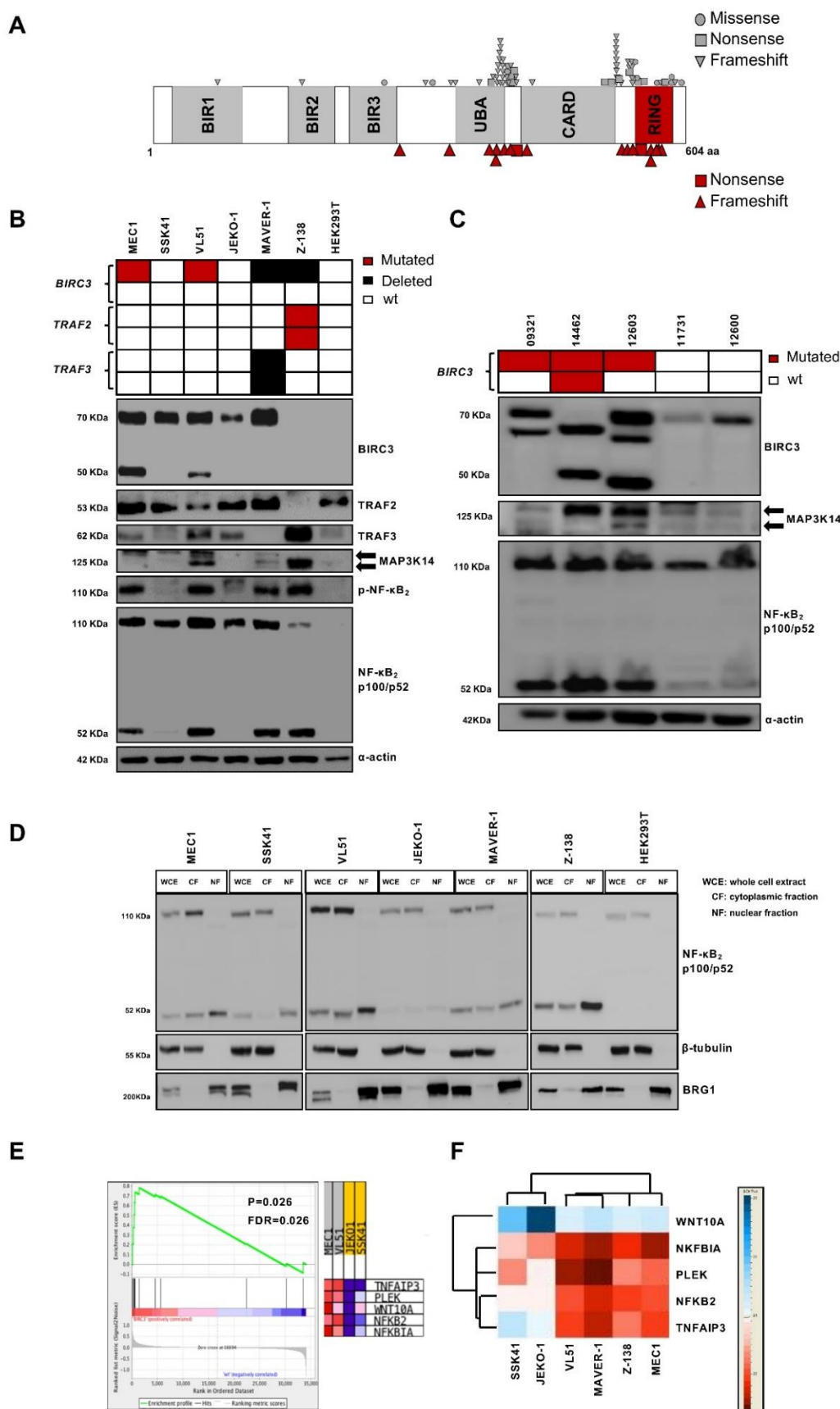


Figure 4: Knockdown of MAP3K14 by RNA interference in VL51 cells.

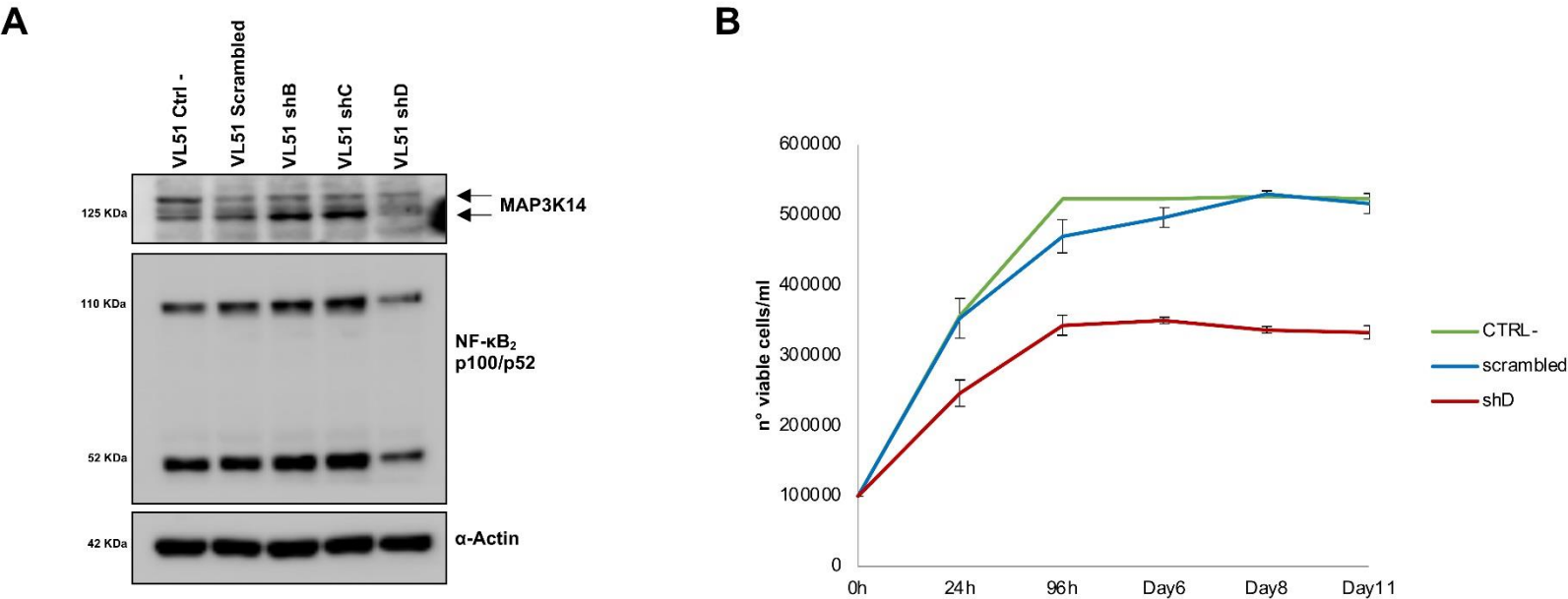


Figure 5: Non-canonical NF- κ B pathway is not switched off by ibrutinib in *BIRC3* mutated cell lines.

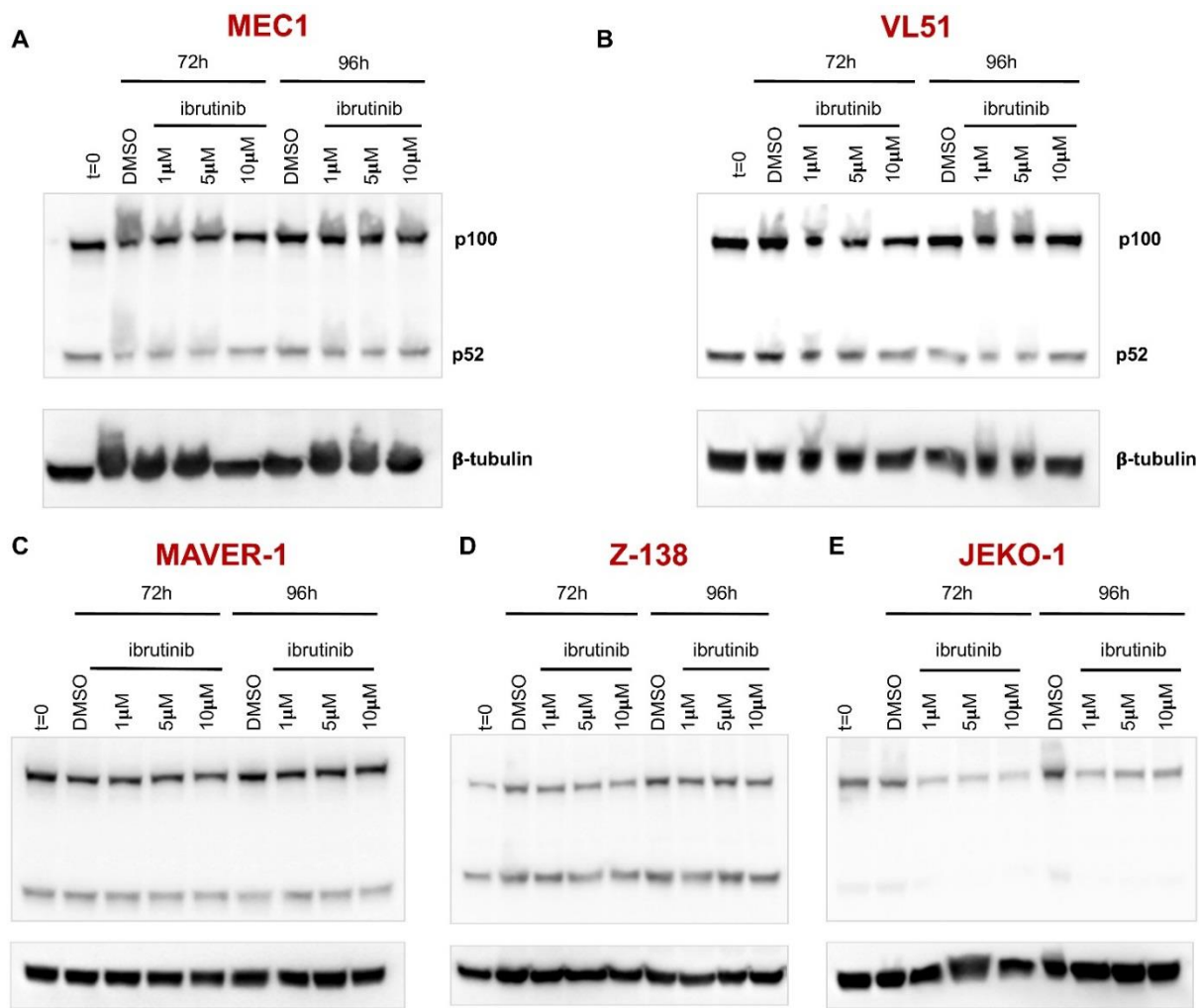
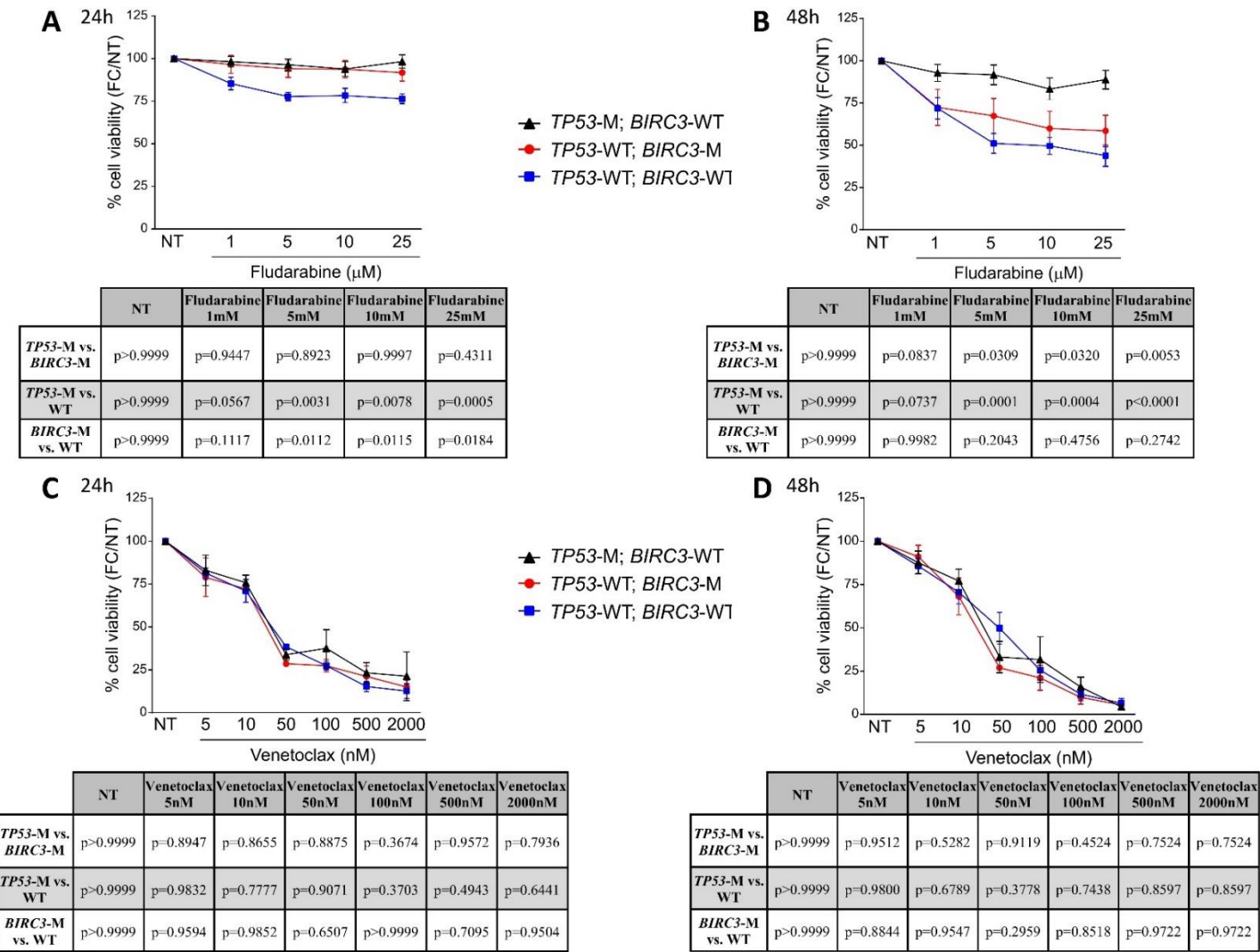


Figure 3

Figure 6: Responses of primary cells lines to fludarabine and venetoclax.



9. SUPPLEMENTARY TABLES

Table S1. Target region

Gene	hg19 chromosome	hg19 coding exon start plus splice site (2bp)	hg19 coding exon stop plus splice site (2bp)
<i>NRAS</i>	chr1	115251156	115251277
	chr1	115252188	115252351
	chr1	115256419	115256601
	chr1	115258669	115258781
<i>XPO1</i>	chr2	61705955	61706103
	chr2	61708318	61708418
	chr2	61709513	61709676
	chr2	61710090	61710228
	chr2	61711070	61711242
	chr2	61712901	61713099
	chr2	61715298	61715408
	chr2	61715721	61715908
	chr2	61717775	61717913
	chr2	61719168	61719335
	chr2	61719458	61719618
	chr2	61719700	61719885
	chr2	61720048	61720190
	chr2	61721027	61721228
	chr2	61722588	61722750
	chr2	61724012	61724144
	chr2	61725806	61725929
	chr2	61725998	61726050
	chr2	61726846	61727031
	chr2	61729129	61729177
	chr2	61729382	61729447
	chr2	61749744	61749820
	chr2	61753553	61753658
	chr2	61760905	61761032
<i>SF3B1</i>	chr2	198257027	198257187
	chr2	198257694	198257914
	chr2	198260778	198261054
	chr2	198262707	198262842
	chr2	198263183	198263307
	chr2	198264777	198264892
	chr2	198264974	198265160
	chr2	198265437	198265662
	chr2	198266122	198266251
	chr2	198266464	198266614
	chr2	198266707	198266856
	chr2	198267278	198267552
	chr2	198267671	198267761
	chr2	198268307	198268490
	chr2	198269798	198269903
	chr2	198269997	198270198
	chr2	198272720	198272845
	chr2	198273091	198273307
	chr2	198274492	198274733

	chr2	198281463	198281637
	chr2	198283231	198283314
	chr2	198285150	198285268
	chr2	198285751	198285859
	chr2	198288530	198288700
	chr2	198299694	198299723
<i>MYD88</i>	chr3	38180153	38180521
	chr3	38181353	38181491
	chr3	38181877	38182061
	chr3	38182246	38182341
	chr3	38182621	38182777
<i>FBXW7</i>	chr4	153244035	153244303
	chr4	153245334	153245548
	chr4	153247156	153247385
	chr4	153249358	153249543
	chr4	153250822	153250939
	chr4	153251882	153252022
	chr4	153253746	153253873
	chr4	153258952	153259090
	chr4	153268080	153268225
	chr4	153271192	153271278
	chr4	153332453	153332955
<i>IRF4</i>	chr6	393150	393370
	chr6	394818	395009
	chr6	395844	395937
	chr6	397105	397254
	chr6	398825	398937
	chr6	401421	401779
	chr6	405015	405132
	chr6	407452	407600
<i>NFKBIE</i>	chr6	44226953	44227023
	chr6	44227777	44228021
	chr6	44228185	44228278
	chr6	44229360	44229587
	chr6	44230294	44230401
	chr6	44232716	44233502
<i>POT1</i>	chr7	124464016	124464130
	chr7	124465304	124465413
	chr7	124467266	124467361
	chr7	124469306	124469398
	chr7	124475331	124475470
	chr7	124481025	124481234
	chr7	124482859	124483019
	chr7	124486994	124487054
	chr7	124491924	124492007
	chr7	124493024	124493194
	chr7	124499009	124499168
	chr7	124503402	124503696
	chr7	124510963	124511097
	chr7	124532318	124532436
	chr7	124537217	124537227
<i>BRAF</i>	chr7	140434397	140434572
	chr7	140439610	140439748
	chr7	140449085	140449220
	chr7	140453073	140453195

	chr7	140453985	140454035
	chr7	140476710	140476890
	chr7	140477789	140477877
	chr7	140481374	140481495
	chr7	140482819	140482959
	chr7	140487346	140487386
	chr7	140494106	140494269
	chr7	140500160	140500283
	chr7	140501210	140501362
	chr7	140507758	140507864
	chr7	140508690	140508797
	chr7	140534407	140534674
	chr7	140549909	140550014
	chr7	140624364	140624503
<i>NOTCH1</i>	chr9	139390512	139392020
<i>NOTCH1_3'UTR</i>	chr9	139388893	139390524
<i>PAX5</i>	chr9	37370906	37371645
	chr9	37033543	37034202
<i>EGR2</i>	chr10	64572967	64574230
	chr10	64575619	64575789
<i>NFKB2</i>	chr10	104155676	104155777
	chr10	104155999	104156101
	chr10	104156155	104156296
	chr10	104156471	104156590
	chr10	104156650	104156822
	chr10	104157048	104157175
	chr10	104157273	104157452
	chr10	104157727	104157852
	chr10	104157958	104158064
	chr10	104158131	104158290
	chr10	104158485	104158631
	chr10	104159034	104159264
	chr10	104159323	104159485
	chr10	104159826	104159961
	chr10	104160024	104160258
	chr10	104160401	104160591
	chr10	104160693	104160816
	chr10	104160926	104161098
	chr10	104161225	104161325
	chr10	104161491	104161684
	chr10	104161794	104161926
	chr10	104161998	104162143
<i>ATM</i>	chr11	108098352	108098425
	chr11	108098501	108098617
	chr11	108099903	108100052
	chr11	108106395	108106563
	chr11	108114678	108114847
	chr11	108115513	108115755
	chr11	108117689	108117856
	chr11	108119658	108119831
	chr11	108121426	108121801
	chr11	108122562	108122760
	chr11	108123542	108123641
	chr11	108124539	108124768
	chr11	108126940	108127069

	chr11	108128206	108128335
	chr11	108129711	108129804
	chr11	108137896	108138071
	chr11	108139135	108139338
	chr11	108141789	108141875
	chr11	108141976	108142135
	chr11	108143257	108143336
	chr11	108143447	108143581
	chr11	108150216	108150337
	chr11	108151720	108151897
	chr11	108153435	108153608
	chr11	108154952	108155202
	chr11	108158325	108158444
	chr11	108159702	108159832
	chr11	108160327	108160530
	chr11	108163344	108163522
	chr11	108164038	108164206
	chr11	108165652	108165788
	chr11	108168012	108168111
	chr11	108170439	108170614
	chr11	108172373	108172518
	chr11	108173578	108173758
	chr11	108175400	108175581
	chr11	108178622	108178713
	chr11	108180885	108181044
	chr11	108183136	108183227
	chr11	108186548	108186640
	chr11	108186736	108186842
	chr11	108188098	108188250
	chr11	108190679	108190787
	chr11	108192026	108192149
	chr11	108196035	108196273
	chr11	108196783	108196954
	chr11	108198370	108198487
	chr11	108199746	108199967
	chr11	108200939	108201150
	chr11	108202169	108202286
	chr11	108202604	108202766
	chr11	108203487	108203629
	chr11	108204611	108204697
	chr11	108205694	108205838
	chr11	108206570	108206690
	chr11	108213947	108214100
	chr11	108216468	108216637
	chr11	108218004	108218094
	chr11	108224491	108224609
	chr11	108225536	108225603
	chr11	108235807	108235947
	chr11	108236050	108236235
<i>BIRC3</i>	chr11	102195241	102196095
	chr11	102196195	102196298
	chr11	102198781	102198863
	chr11	102199626	102199678
	chr11	102201728	102201974
	chr11	102206695	102206953

	chr11	102207489	102207534
	chr11	102207638	102207833
<i>KRAS</i>	chr12	25368375	25368496
	chr12	25378546	25378709
	chr12	25380166	25380348
	chr12	25398206	25398318
<i>MAP2K1</i>	chr15	66679683	66679767
	chr15	66727362	66727577
	chr15	66729081	66729232
	chr15	66735615	66735697
	chr15	66736991	66737047
	chr15	66774090	66774219
	chr15	66777325	66777531
	chr15	66779563	66779632
	chr15	66781550	66781616
	chr15	66782053	66782103
	chr15	66782837	66782955
<i>MGA</i>	chr15	41961082	41962166
	chr15	41988262	41989231
	chr15	41991040	41991149
	chr15	41991251	41991367
	chr15	41999915	42000067
	chr15	42000291	42000416
	chr15	42002878	42003557
	chr15	42005338	42005704
	chr15	42019367	42019614
	chr15	42021351	42021557
	chr15	42026699	42026802
	chr15	42028368	42028906
	chr15	42032240	42032411
	chr15	42034733	42035380
	chr15	42040824	42041135
	chr15	42041298	42042823
	chr15	42046624	42046775
	chr15	42049955	42050057
	chr15	42052510	42052737
	chr15	42053926	42054058
	chr15	42054316	42054570
	chr15	42057073	42057270
	chr15	42058191	42059488
<i>TP53</i>	chr17	7572927	7573010
	chr17	7573925	7574035
	chr17	7576851	7576928
	chr17	7577017	7577157
	chr17	7577497	7577610
	chr17	7578175	7578291
	chr17	7578369	7578556
	chr17	7579310	7579592
	chr17	7579698	7579723
	chr17	7579837	7579912
<i>IKZF3</i>	chr17	37922032	37922756
	chr17	37933893	37934030
	chr17	37944500	37944637
	chr17	37947658	37947846
	chr17	37948915	37949196

	chr17	37985629	37985751
	chr17	37988320	37988434
	chr17	38020322	38020429
<i>RPS15</i>	chr19	1438374	1438477
	chr19	1438785	1438911
	chr19	1440007	1440262
	chr19	1440337	1440471
<i>SAMHD1</i>	chr20	35521335	35521471
	chr20	35526223	35526364
	chr20	35526841	35526949
	chr20	35532558	35532654
	chr20	35533765	35533908
	chr20	35539619	35539738
	chr20	35540862	35540957
	chr20	35545123	35545235
	chr20	35545350	35545454
	chr20	35547765	35547924
	chr20	35555583	35555657
	chr20	35559161	35559280
	chr20	35563430	35563594
	chr20	35569440	35569516
	chr20	35575139	35575209
	chr20	35579837	35580046
<i>ASXL1</i>	chr20	30946548	30946665
	chr20	30954176	30954279
	chr20	30955479	30955582
	chr20	30956807	30956936
	chr20	31015920	31016061
	chr20	31016117	31016235
	chr20	31017130	31017244
	chr20	31017693	31017866
	chr20	31019113	31019297
	chr20	31019375	31019492
	chr20	31020672	31020798
	chr20	31021076	31021730
	chr20	31022224	31025151
<i>ZMYM3</i>	chrX	70460766	70460960
	chrX	70461075	70461196
	chrX	70462018	70462276
	chrX	70462818	70462936
	chrX	70463677	70463832
	chrX	70464150	70464322
	chrX	70464638	70464745
	chrX	70465187	70465337
	chrX	70465516	70465694
	chrX	70465834	70465950
	chrX	70466201	70466364
	chrX	70466443	70466544
	chrX	70467193	70467362
	chrX	70467582	70467758
	chrX	70468010	70468164
	chrX	70468286	70468376
	chrX	70468534	70468653
	chrX	70468867	70469021
	chrX	70469309	70469531

	chrX	70469874	70470055
	chrX	70470280	70470578
	chrX	70471026	70471096
	chrX	70471406	70471453
	chrX	70472437	70473105

Table S2. Target region with $\geq 1000X$ and $\geq 2000X$ coverage

Material	Sample ID	Target Region Coverage (%)	
		$\geq 1000X$	$\geq 2000X$
RNA	3389	29.6	19.9
RNA	3390	49.8	28
RNA	3392	86.8	31.1
RNA	3393	55.2	33.6
RNA	3394	58.6	37.5
RNA	3395	91.7	38.8
RNA	3396	62	39.5
gDNA	4822	66.5	44.5
gDNA	4937	88.2	46.7
gDNA	4997	92.3	88.2
gDNA	5564	67.6	49
gDNA	5868	86	58
gDNA	6415	92.6	64
gDNA	7274	91	67.4
gDNA	7302	86.5	73.8
gDNA	8461	98.3	74.5
gDNA	9248	98.4	74.5
gDNA	9289	95.9	75.1
gDNA	9291	89.7	75.2
gDNA	10676	100	99.9
gDNA	10851	89.2	75.4
gDNA	12162	98.3	76.3
gDNA	12640	98.9	90.2
gDNA	12955	99.8	97.4
gDNA	13318	99.9	99.2
gDNA	13426	66.4	46.5
gDNA	13443	72.2	40.7
gDNA	14261	90.2	78
gDNA	14293	95.8	78.9
gDNA	14419	94.2	79.3
gDNA	14462	99.9	96.3
gDNA	14687	100	99.8
gDNA	14821	69.6	40.3
gDNA	14830	75.4	31.6
gDNA	15065	99.7	79.5
gDNA	15257	97.8	79.6
gDNA	15280	98.3	80
gDNA	15361	95.7	80.7
gDNA	15367	95.6	80.9
gDNA	15426	87.8	80.9
gDNA	15448	68.7	39.2
gDNA	15467	96.2	82.5
gDNA	15505	96.3	82.8
gDNA	15522	96.7	83.6
gDNA	15537	97.8	83.7
gDNA	15562	96.5	83.7
gDNA	15597	93.8	84.6
gDNA	15871	98.5	84.8
gDNA	15891	97.5	85
gDNA	15997	91.3	85.6

gDNA	16243	99.9	98.8
gDNA	17548	99.6	97.4
gDNA	17698	86.6	68
gDNA	18723	97.7	86
gDNA	18736	98.1	86.2
gDNA	19184	97.5	86.5
gDNA	19189	97	87
gDNA	19363	86.9	74.3
gDNA	19402	99.7	97.9
gDNA	19405	100	99.6
gDNA	19533	98.2	87
gDNA	20010	98.6	87.3
gDNA	20196	90.1	87.6
gDNA	20802	98.1	87.8
gDNA	20803	98.2	88
gDNA	20804	99.1	91.2
gDNA	20805	98.6	90.3
gDNA	20806	98.2	89.1
gDNA	20807	98.4	90.1
gDNA	20808	96.2	89.4
gDNA	20809	96.3	89.7
gDNA	20810	99.8	91.1
gDNA	20811	98.4	90.5
gDNA	20812	95.0	90.1
gDNA	20813	98.6	90.4
gDNA	20814	98.4	90.4
gDNA	20815	99.1	90.7
gDNA	20816	99.2	90.9
gDNA	20817	95.6	91.2
gDNA	20818	99.4	91.7
gDNA	20819	98.4	91.7
gDNA	20820	98.8	92.3
gDNA	20821	98.8	92.3
gDNA	20822	98.2	92.5
gDNA	20823	99.3	92.8
gDNA	20824	98.9	92.9
gDNA	20825	99.3	93.1
gDNA	20826	98.7	93.3
gDNA	20827	98.1	93.4
gDNA	20828	99.8	93.4
gDNA	20829	99	93.5
gDNA	20830	98.2	93.7
gDNA	20831	98.9	93.7
gDNA	20832	99.2	93.8
gDNA	20833	99	93.9
gDNA	20834	99.5	94.5
gDNA	20835	99.3	94.6
gDNA	20844	99.3	94.7
gDNA	20845	98.4	94.9
gDNA	20846	99.4	95.3
gDNA	20847	99.9	95.4
gDNA	20848	99.1	95.4
gDNA	20849	99.4	95.4
gDNA	20850	98.8	95.4
gDNA	20851	99.2	95.6

gDNA	20852	99.2	95.6
gDNA	20853	99.7	95.9
gDNA	20854	99.7	95.9
gDNA	20855	99	96.1
gDNA	20856	99.2	96.1
gDNA	20857	99.4	96.2
gDNA	20858	99.4	96.3
gDNA	20859	99.9	96.5
gDNA	20860	99.8	96.5
gDNA	20861	99.4	96.6
gDNA	20864	99.4	96.6
gDNA	20865	99.1	96.7
gDNA	20866	99.7	96.7
gDNA	20867	99.3	96.8
gDNA	20868	99.4	96.8
gDNA	20869	99.8	96.8
gDNA	20870	99.6	96.8
gDNA	20871	99.1	96.9
gDNA	20872	99.3	96.9
gDNA	20873	99.1	96.9
gDNA	20874	99.9	97
gDNA	20875	99.4	97.1
gDNA	20876	99.2	97.1
gDNA	20896	99.4	97.1
gDNA	20897	99.1	97.2
gDNA	21006	99.4	97.2
gDNA	21007	99.6	97.2
gDNA	21008	99.3	97.2
gDNA	21009	99.4	97.3
gDNA	21010	99.4	97.3
gDNA	21011	99.1	97.3
gDNA	21012	99.2	97.3
gDNA	21013	99.5	97.3
gDNA	21014	99.4	97.4
gDNA	21015	99.6	97.4
gDNA	21016	99.3	97.4
gDNA	21017	99.2	97.4
gDNA	21018	99.3	97.4
gDNA	21019	99.3	97.5
gDNA	21020	99.5	97.5
gDNA	21021	99.4	97.5
gDNA	21022	99.2	97.5
gDNA	21045	99.2	97.6
gDNA	21046	99.6	97.6
gDNA	21047	99.4	97.6
gDNA	21048	99.5	97.6
gDNA	21049	99.4	97.7
gDNA	21050	99.3	97.7
gDNA	21051	99.5	97.7
gDNA	21052	99.6	97.7
gDNA	21053	99.6	97.7
gDNA	21054	99.5	97.8
gDNA	21095	99.9	97.8
gDNA	21096	99.6	97.8
gDNA	21097	99.4	97.8

gDNA	21098	99.6	97.8
gDNA	21099	99.4	97.8
gDNA	21189	99.5	97.8
gDNA	21190	99.5	97.8
gDNA	21191	99.4	98
gDNA	21193	99.8	98
gDNA	21194	99.7	98
gDNA	21195	99.7	98
gDNA	21196	99.5	98
gDNA	21197	99.4	98.1
gDNA	21198	99.6	98.1
gDNA	21199	99.5	98.1
gDNA	21291	99.7	98.1
gDNA	21292	99.5	98.1
gDNA	21293	99.6	98.1
gDNA	21294	99.8	98.2
gDNA	21295	99.7	98.2
gDNA	21296	99.6	98.2
gDNA	21297	99.8	98.2
gDNA	21299	99.8	98.2
gDNA	21300	99.5	98.3
gDNA	21301	99.6	98.3
gDNA	21302	99.8	98.3
gDNA	21303	99.5	98.3
gDNA	21304	99.5	98.3
gDNA	21305	99.9	98.3
gDNA	21306	99.6	98.4
gDNA	21307	99.7	98.4
gDNA	21308	99.6	98.4
gDNA	21309	99.8	98.4
gDNA	23050	99.7	98.4
gDNA	23051	99.6	98.5
gDNA	23052	99.7	98.5
gDNA	23053	99.9	98.5
gDNA	23054	99.6	98.5
gDNA	23055	99.8	98.5
gDNA	23056	99.9	98.5
gDNA	23057	99.6	98.5
gDNA	23058	99.8	98.5
gDNA	23059	99.8	98.5
gDNA	23060	99.9	98.6
gDNA	23061	99.8	98.6
gDNA	23062	99.7	98.6
gDNA	23063	99.6	98.6
gDNA	23064	99.7	98.6
gDNA	23065	99.7	98.7
gDNA	23066	99.7	98.7
gDNA	23067	99.6	98.7
gDNA	23068	99.9	98.7
gDNA	23069	99.8	98.7
gDNA	23070	99.9	98.7
gDNA	23071	99.6	98.7
gDNA	23072	100	98.7
gDNA	23073	99.9	98.7
gDNA	23074	99.7	98.7

gDNA	23075	99.9	98.7
gDNA	23076	99.9	98.8
gDNA	23077	99.7	98.8
gDNA	23078	99.7	98.8
gDNA	23079	99.6	98.8
gDNA	23080	99.9	98.8
gDNA	23081	99.9	98.8
gDNA	23082	99.8	98.8
gDNA	23083	99.9	98.8
gDNA	23084	99.9	98.8
gDNA	23085	99.9	98.9
gDNA	23086	99.9	98.9
gDNA	23087	99.9	98.9
gDNA	23088	99.9	98.9
gDNA	23089	99.9	98.9
gDNA	23090	99.9	98.9
gDNA	23091	99.7	98.9
gDNA	23092	99.5	98.9
gDNA	23093	99.8	98.9
gDNA	23094	99.7	98.9
gDNA	23095	99.9	98.9
gDNA	23096	99.9	98.9
gDNA	23097	99.9	98.9
gDNA	23098	99.9	98.9
gDNA	23099	99	99
gDNA	23100	99.9	99
gDNA	23101	99.7	99
gDNA	23102	99.9	99
gDNA	23103	99.9	99
gDNA	23104	99.9	99
gDNA	23105	99.9	99
gDNA	23106	99.7	99.1
gDNA	23107	99.9	99.1
gDNA	23108	99.9	99.1
gDNA	23109	99.9	99.1
gDNA	23110	99.9	99.1
gDNA	23111	99.9	99.1
gDNA	23112	99.9	99.1
gDNA	23113	99.9	99.1
gDNA	23114	99.9	99.1
gDNA	23115	99.8	99.1
gDNA	23116	99.9	99.1
gDNA	23117	99.9	99.1
gDNA	23118	99.9	99.2
gDNA	23119	99.9	99.2
gDNA	23120	99	99.2
gDNA	23121	99.9	99.2
gDNA	23122	99.8	99.2
gDNA	23123	99.9	99.2
gDNA	23124	99.9	99.3
gDNA	23125	99.9	99.3
gDNA	23126	99.9	99.3
gDNA	23127	99.9	99.4
gDNA	23128	99.9	99.4
gDNA	23129	99.9	99.4

gDNA	23130	99.9	99.4
gDNA	23131	99.9	99.4
gDNA	23132	99.9	99.4
gDNA	23133	99.9	99.4
gDNA	23134	99.9	99.5
gDNA	23135	99.9	99.5
gDNA	23136	99.8	99.5
gDNA	23137	99.9	99.5
gDNA	23138	100	99.5
gDNA	23139	99.9	99.5
gDNA	23140	100	99.6
gDNA	23141	100	99.6
gDNA	23142	99.9	99.6
gDNA	23143	99.9	99.6
gDNA	23144	100	99.8
gDNA	23145	100	99.9
gDNA	23146	100	99.9

Table S3. Somatic non-synonymous mutations discovered in tumor samples

ID Sample	Gene	RefSeq	#CHROM	POS	REF	VAR	cDNA	AA	VAf in tumor samples
3392	<i>NOTCH1</i>	NM_017617.3	chr9	139390648	CAG	C	c.7541_7542delCT	p.P2514fs*4	34.4 (386/1119)
3396	<i>TP53</i>	NM_000546.5	chr17	7577610	T	TC	c.673-2A>G	-	5.13 (44/857)
4822	<i>NOTCH1</i>	NM_017617.3	chr9	139390648	CAG	C	c.7541_7542delCT	p.P2514fs*4	36 (581/1614)
4937	<i>SF3B1</i>	NM_012433.2	chr2	198267371	G	T	c.1986C>A	p.H662Q	31.15 (3202/10278)
4997	<i>TP53</i>	NM_000546.5	chr17	7578394	T	A	c.536A>T	p.H179L	89.57 (2233/2491)
5564	<i>ATM</i>	NM_000051.3	chr11	108206593	G	A	c.8173G>A	p.D2725N	18.78 (496/2641)
5564	<i>ATM</i>	NM_000051.3	chr11	108224528	C	T	c.8707C>T	p.P2903S	23.06 (751/3257)
5564	<i>POT1</i>	NM_015450.2	chr7	124493080	C	A	c.422G>T	p.G272V	15.23 (545/3579)
7302	<i>NOTCH1</i>	NM_017617.3	chr9	139390759	CG	C	c.7431_7431delC	p.A2478fs*5	43.4 (447/1030)
10676	<i>BRAF</i>	NM_004333.4	chr7	140534588	A	T	c.325T>A	p.F109I	40.4 (5204/12861)
10676	<i>SF3B1</i>	NM_012433.2	chr2	198266834	T	C	c.2098A>G	p.K700E	20.3 (2415/11876)
12162	<i>MGA</i>	NM_001164273.1	chr15	41989130	A	AT	c.1922_1923insT	p.T642fs*15	11.59 (361/3115)
12162	<i>NOTCH1</i>	NM_017617.3	chr9	139390648	CAG	C	c.7541_7542delCT	p.P2514fs*4	41.64 (513/1232)
12955	<i>FBXW7</i>	NM_033632	chr4	153258983	G	A	c.832C>T	p.R278*	15.86 (550/3467)
13443	<i>BIRC3</i>	NM_001165.4	chr11	102207656	AC	A	c.1639_1639delC	p.Q547fs*21	10.5 (55/523)
14293	<i>TP53</i>	NM_000546.5	chr17	7578553	T	C	c.377A>G	p.Y126C	13.65 (731/5353)
14419	<i>ATM</i>	NM_000051.3	chr11	108170513	AT	A	c.5079_5079delT	p.D1693fs*21	86.18 (2014/2332)
14419	<i>MGA</i>	NM_001164273.1	chr15	42054328	TAA	T	c.7513_7514delAA	p.K2504fs*31	36.5 (803/2199)
14419	<i>NFKBIE</i>	NM_004556.2	chr6	44232738	TGTAA	T	c.759_762delTTAC	p.Y254fs*13	21 (285/1355)
14419	<i>NOTCH1</i>	NM_017617.3	chr9	139390648	CAG	C	c.7541_7542delCT	p.P2514fs*4	12.79 (169/1320)
14462	<i>BIRC3</i>	NM_001165.4	chr11	102201928	TA	T	c.1281_1281delA	p.R428fs*19	31.17 (944/3028)
14462	<i>BIRC3</i>	NM_001165.4	chr11	102207519	AG	A	c.1609_1609delG	p.E537fs*31	27 (678/2511)
14462	<i>XPO1</i>	NM_003400.3	chr2	61719472	C	T	c.1711G>A	p.E571K	36.9 (1803/4877)
14687	<i>ATM</i>	NM_000051.3	chr11	108201101	C	T	c.7468C>T	p.L2490F	33.8 (5139/15183)
15257	<i>SF3B1</i>	NM_012433.2	chr2	198266611	C	T	c.2225G>A	p.G742D	30.16 (2557/8475)
15257	<i>XPO1</i>	NM_003400.3	chr2	61719472	C	T	c.1711G>A	p.E571K	30.4 (2882/9475)
15280	<i>SF3B1</i>	NM_012433.2	chr2	198266834	T	C	c.2098A>G	p.K700E	18.28 (647/3535)
15361	<i>NOTCH1</i>	NM_017617.3	chr9	139390648	CAG	C	c.7541_7542delCT	p.P2514fs*4	38.84 (3004/7720)
15367	<i>SF3B1</i>	NM_012433.2	chr2	198266834	T	C	c.2098A>G	p.K700E	10.13 (220/2171)
15367	<i>TP53</i>	NM_000546.5	chr17	7577539	G	A	c.742C>T	p.R248W	38.49 (1411/3662)
15448	<i>POT1</i>	NM_015450.2	chr7	124537225	C	CA	c.2_3insT	initiating Methionine lost	27.2 (61/224)
15448	<i>TP53</i>	NM_000546.5	chr17	7578190	T	G	c.659A>C	p.Y220S	23.5 (2002/8499)
15505	<i>KRAS</i>	NM_033360.2	chr12	25398255	G	T	c.64C>A	p.Q22K	21.95 (1222/5559)
15505	<i>SAMHD1</i>	NM_015474	chr20	35526905	CA	C	c.1545_1545delT	p.I515fs*35	43.16 (3089/5442)

15505	<i>SAMHD1</i>	NM_015474	chr20	35526278	C	T	c.1693G>A	p.A565T	50.02 (3232/6457)
15505	<i>TP53</i>	NM_000546.5	chr17	7577548	C	T	c.733G>A	p.G245S	19.95 (979/4903)
15537	<i>BIRC3</i>	NM_001165.4	chr11	102201966	G	GA	c.1318_1319insA	p.S441fs*3	10.34 (156/1505)
15537	<i>BIRC3</i>	NM_001165.4	chr11	102201960	G	T	c.1312G>T	p.E438*	11.79 (186/1586)
15537	<i>BIRC3</i>	NM_001165.4	chr11	102207656	AC	A	c.1639_1639delC	p.Q547fs*21	20.99 (390/1853)
15597	<i>SF3B1</i>	NM_012433.2	chr2	198267484	G	A	c.1873C>T	p.R625C	10.8 (677/6265)
15597	<i>TP53</i>	NM_000546.5	chr17	7577610	T	C	c.673-2A>G	-	22.44 (724/3227)
15891	<i>TP53</i>	NM_000546.5	chr17	7579372	GC	G	c.314_314delG	p.G105fs*18	18.41 (648/3505)
15891	<i>TP53</i>	NM_000546.5	chr17	7577610	T	A	c.673-2A>G	-	33.55 (787/2208)
16243	<i>ATM</i>	NM_000051.3	chr11	108160350	C	T	c.4258C>T	p.L1420F	31.7 (2184/6880)
16243	<i>SF3B1</i>	NM_012433.2	chr2	198267489	T	C	c.1868A>G	p.Y623C	16.9 (1066/6299)
17698	<i>NOTCH1</i>	NM_017617.3	chr9	139390800	AG	A	c.7390_7390delC	p.L2464fs*13	44.2 (1955/4422)
18723	<i>TP53</i>	NM_000546.5	chr17	7578208	T	C	c.641A>G	p.H214R	7.01 (502/7158)
18736	<i>FBXW7</i>	NM_033632.3	chr4	153253770	C	T	c.963G>A	p.W321*	23.23 (1103/4742)
18736	<i>IRF4</i>	NM_002460.3	chr6	394951	T	G	c.347T>G	p.L116R	14.58 (1202/8245)
19184	<i>ZMYM3</i>	NM_201599	chrX	70472961	CA	C	c.144_144delT	p.G49fs*64	18.86 (458/2423)
19363	<i>SF3B1</i>	NM_012433.2	chr2	198267359	C	G	c.1998G>C	p.K666N	26.67 (1767/6625)
19363	<i>XPO1</i>	NM_003400.3	chr2	61719186	T	C	c.1871A>G	p.D624G	28.31 (1129/3987)
19405	<i>NOTCH1</i>	NM_017617.3	chr9	139390585	C	T	c.7606G>A	p.V2536I	32.98 (6297/19088)
19533	<i>XPO1</i>	NM_003400.3	chr2	61719472	C	T	c.1711G>A	p.E571K	44.82 (3115/6948)
20010	<i>SF3B1</i>	NM_012433.2	chr2	198266822	T	A	c.2110A>T	p.I704F	12.14 (753/6200)
20010	<i>SF3B1</i>	NM_012433.2	chr2	198267371	G	T	c.1986C>A	p.H662Q	15.4 (686/4454)
20010	<i>TP53</i>	NM_000546.5	chr17	7578413	C	G	c.517G>C	p.V173L	11.54 (261/2260)
20196	<i>IKZF3</i>	NM_012481.4	chr17	37985732	G	A	c.71C>T	p.A24V	51.19 (2296/4484)
20802	<i>NOTCH1</i>	NM_017617.3	chr9	139390648	CAG	C	c.7541_7542delCT	p.P2514fs*4	37.13 (822/2209)
20803	<i>NOTCH1</i>	NM_017617.3	chr9	139390648	CAG	C	c.7541_7542delCT	p.P2514fs*4	23.3 (916/3923)
20804	<i>IKZF3</i>	NM_012481.4	chr17	37947776	A	C	c.485T>G	p.L162R	27.22 (1316/4834)
20804	<i>ZMYM3</i>	NM_201599	chrX	70472962	AG	A	c.143_143delC	p.P48fs*65	24.43 (579/2369)
20807	<i>MYD88</i>	NM_002468.4	chr3	38182641	T	C	c.794T>C	p.L265P	21.99 (1087/4940)
20808	<i>SF3B1</i>	NM_012433.2	chr2	198267360	T	G	c.1997A>C	p.K666T	22.11 (1782/8056)
20810	<i>NOTCH1</i>	NM_017617.3	chr9	139390648	CAG	C	c.7541_7542delCT	p.P2514fs*4	34.54 (1636/4731)
20811	<i>SF3B1</i>	NM_012433.2	chr2	198266713	C	T	c.2219G>A	p.G740E	10.96 (424/3865)
20812	<i>IKZF3</i>	NM_012481.4	chr17	37947776	A	C	c.485T>G	p.L162R	42.39 (3787/8922)
20812	<i>NOTCH1</i>	NM_017617.3	chr9	139390975	G	A	c.7216C>T	p.Q2406*	41.51 (2956/7119)
20812	<i>RPS15</i>	NM_001018.3	chr19	1440439	C	T	c.413C>T	p.S138F	14.08 (309/2187)
20813	<i>MGA</i>	NM_001164273.1	chr15	42028793	TA	T	c.4332_4332delA	p.L1444fs*36	32.37 (1714/5295)
20818	<i>ASXL1</i>	NM_015338.5	chr20	31024704	G	A	c.4189G>A	p.G1397S	48.02 (2053/4270)
20820	<i>XPO1</i>	NM_003400.3	chr2	61719472	C	A	c.1711G>T	p.E571*	10.68 (240/2247)
20821	<i>BRAF</i>	NM_004333.4	chr7	140481402	C	G	c.1406G>C	p.G469A	35.17 (1666/4732)

20821	<i>EGR2</i>	NM_000399.3	chr10	64573167	C	G	c.1231G>C	p.D411H	34.43 (2156/6253)
20822	<i>ATM</i>	NM_000051.3	chr11	108126954	GA	G	c.2138_2138delA	p.T713fs*20	10.87 (332/3055)
20822	<i>BIRC3</i>	NM_001165.4	chr11	102201945	GAA	G	c.1298_1299delAA	p.R434fs*3	10.88 (420/3857)
20822	<i>IRF4</i>	NM_002460.3	chr6	394951	T	G	c.347T>G	p.L116R	29.37 (1664/5661)
20823	<i>NOTCH1</i>	NM_017617.3	chr9	139390648	CAG	C	c.7541_7542delCT	p.P2514fs*4	25.53 (1971/5742)
20827	<i>IKZF3</i>	NM_012481.4	chr17	37947776	A	C	c.485T>G	p.L162R	41.37 (1814/4377)
20831	<i>ATM</i>	NM_000051.3	chr11	108178641	CG	C	c.5693_5693delG	p.R1898fs*19	11.94 (151/1265)
20832	<i>ATM</i>	NM_000051.3	chr11	108175463	A	T	c.5558A>T	p.D1853V	50.28 (2634/5237)
20832	<i>XPO1</i>	NM_003400.3	chr2	61719472	C	T	c.1711G>A	p.E571K	44.23 (2407/5441)
20833	<i>BIRC3</i>	NM_001165.4	chr11	102207704	CA	C	c.1687_1687delA	p.E564fs*4	17.15 (996/5794)
20833	<i>ZMYM3</i>	NM_201599	chrX	70472444	A	T	c.662T>A	p.L221*	85.83 (1950/2268)
20834	<i>KRAS</i>	NM_033360.2	chr12	25398262	C	G	c.57G>C	p.L19F	28.85 (1123/3893)
20844	<i>TP53</i>	NM_000546.5	chr17	7579419	AG	A	c.267_267delC	p.S90fs*33	3.16 (86/2723)
20845	<i>NOTCH1</i>	NM_017617.3	chr9	139390648	CAG	C	c.7541_7542delCT	p.P2514fs*4	10.23 (424/4132)
20845	<i>RPS15</i>	NM_001018.3	chr19	1440436	C	T	c.413C>T	p.S138F	22.71 (422/1857)
20845	<i>XPO1</i>	NM_003400.3	chr2	61719186	T	C	c.1871A>G	p.D624G	38.73 (2087/5385)
20846	<i>TP53</i>	NM_000546.5	chr17	7578176	C	T	c.672+1G>A	-	28.1 (726/2584)
20847	<i>BRAF</i>	NM_004333.4	chr7	140453136	A	T	c.1799T>A	p.V600E	17.69 (820/4633)
20849	<i>SF3B1</i>	NM_012433.2	chr2	198267359	C	A	c.1998G>T	p.K666N	20.2 (1033/5110)
20850	<i>SF3B1</i>	NM_012433.2	chr2	198266834	T	C	c.2098A>G	p.K700E	12.16 (460/3779)
20852	<i>ATM</i>	NM_000051.3	chr11	108143456	C	G	c.3161C>G	p.P1054R	48.39 (4558/9414)
20852	<i>NFKBIE</i>	NM_004556.2	chr6	44232738	TGTAA	T	c.759_762delTTAC	p.Y254fs*13	81.93 (3260/3973)
20852	<i>SF3B1</i>	NM_012433.2	chr2	198266834	T	C	c.2098A>G	p.K700E	13.94 (718/5150)
20853	<i>ATM</i>	NM_000051.3	chr11	108143456	C	G	c.3161C>G	p.P1054R	51.51 (2525/4894)
20853	<i>BIRC3</i>	NM_001165.4	chr11	102207684	AC	A	c.1667_1667delC	p.T556fs*12	49.27 (2360/4789)
20853	<i>SF3B1</i>	NM_012433.2	chr2	198266611	C	T	c.2225G>A	p.G742D	43.96 (1797/4083)
20855	<i>NFKBIE</i>	NM_004556.2	chr6	44232738	TGTAA	T	c.759_762delTTAC	p.Y254fs*13	13.6 (507/3712)
20857	<i>EGR2</i>	NM_000399.3	chr10	64573248	G	T	c.1150C>A	p.H384N	27.07 (1313/4848)
20857	<i>NOTCH1</i>	NM_017617.3	chr9	139390648	CAG	C	c.7541_7542delCT	p.P2514fs*4	41.62 (1463/3505)
20860	<i>MGA</i>	NM_001164273.1	chr15	42028430	AT	A	c.3969_3969delT	p.Y1323*	22.38 (1126/5032)
20860	<i>TP53</i>	NM_000546.5	chr17	7577123	A	C	c.815T>G	p.V272G	5.11 (248/4847)
20861	<i>EGR2</i>	NM_000399.3	chr10	64573248	G	T	c.1150C>A	p.H384N	10.1 (720/7121)
20861	<i>NOTCH1</i>	NM_017617.3	chr9	139390648	CAG	C	c.7541_7542delCT	p.P2514fs*4	23.64 (1042/4396)
20868	<i>SF3B1</i>	NM_012433.2	chr2	198267360	T	G	c.1997A>C	p.K666T	19.46 (1184/6077)
20868	<i>SF3B1</i>	NM_012433.2	chr2	198267361	T	C	c.1996A>G	p.K666E	20.3 (1249/6152)
20870	<i>ATM</i>	NM_000051.3	chr11	108160480	T	G	c.4388T>G	p.F1463C	49.82 (3142/6305)
20872	<i>NOTCH1</i>	NM_017617.3	chr9	139390648	CAG	C	c.7541_7542delCT	p.P2514fs*4	14.06 (532/3781)
20872	<i>TP53</i>	NM_000546.5	chr17	7577108	C	A	c.830G>T	p.C277F	5.21 (344/6605)
20875	<i>XPO1</i>	NM_003400.3	chr2	61719471	T	C	c.1712A>G	p.E571G	20.02 (1086/5420)

20876	<i>SF3B1</i>	NM_012433.2	chr2	198267361	T	C	c.1996A>G	p.K666E	41.44 (2390/5766)
20897	<i>BIRC3</i>	NM_001165.4	chr11	102207656	AC	A	c.1639_1639delC	p.Q547fs*21	75.16 (838/1115)
21007	<i>NOTCH1</i>	NM_017617.3	chr9	139390648	CAG	C	c.7541_7542delCT	p.P2514fs*4	30.48 (1704/5585)
21007	<i>TP53</i>	NM_000546.5	chr17	7578460	A	T	c.470T>A	p.V157D	6.84 (511/7466)
21008	<i>SF3B1</i>	NM_012433.2	chr2	198266709	C	A	c.2223G>T	p.K741N	10.72 (452/4217)
21010	<i>IRF4</i>	NM_002460.3	chr6	394951	T	G	c.347T>G	p.L116R	54.95 (2315/4210)
21010	<i>NOTCH1</i>	NM_017617.3	chr9	139390648	CAG	C	c.7541_7542delCT	p.P2514fs*4	33.41 (449/1340)
21011	<i>BRAF</i>	NM_004333.4	chr7	140481402	C	G	c.1406G>C	p.G469A	41.92 (1971/4693)
21012	<i>FBXW7</i>	NM_033632.3	chr4	153247289	G	A	c.1513C>T	p.R505C	42.2 (1834/4342)
21012	<i>NOTCH1</i>	NM_017617.3	chr9	139391200	C	CCACA	c.6990_6991insTGTG	p.A2331fs*24	30.69 (421/1353)
21012	<i>TP53</i>	NM_000546.5	chr17	7578535	T	A	c.395A>T	p.K132M	7.85 (244/3109)
21013	<i>SF3B1</i>	NM_012433.2	chr2	198266611	C	T	c.2225G>A	p.G742D	13.18 (653/4951)
21014	<i>NOTCH1</i>	NM_017617.3	chr9	139390648	CAG	C	c.7541_7542delCT	p.P2514fs*4	20.25 (873/4302)
21015	<i>NOTCH1</i>	NM_017617.3	chr9	139390648	CAG	C	c.7541_7542delCT	p.P2514fs*4	46.48 (1517/3261)
21015	<i>SF3B1</i>	NM_012433.2	chr2	198266821	A	T	c.2111T>A	p.I704N	47.02 (2466/5244)
21015	<i>TP53</i>	NM_000546.5	chr17	7577117	A	T	c.821T>A	p.V274D	16.17 (876/5410)
21015	<i>XPO1</i>	NM_003400.3	chr2	61719472	C	T	c.1711G>A	p.E571K	13.72 (811/5912)
21016	<i>NOTCH1</i>	NM_017617.3	chr9	139390648	CAG	C	c.7541_7542delCT	p.P2514fs*4	14.06 (532/3781)
21017	<i>ATM</i>	NM_000051.3	chr11	108143456	C	G	c.3161C>G	p.P1054R	78.34 (3292/4200)
21017	<i>IKZF3</i>	NM_012481.4	chr17	37985732	G	A	c.71C>T	p.A24V	47.79 (3051/6380)
21018	<i>TP53</i>	NM_000546.5	chr17	7578400	G	A	c.530C>T	p.P177L	5.38 (288/5353)
21018	<i>XPO1</i>	NM_003400.3	chr2	61719472	C	T	c.1711G>A	p.E571K	22.72 (2210/9718)
21019	<i>FBXW7</i>	NM_033632.3	chr4	153245446	G	A	c.1745C>T	p.S582L	17.19 (1314/7640)
21019	<i>TP53</i>	NM_000546.5	chr17	7577548	C	A	c.733G>T	p.G245C	3.19 (199/6226)
21019	<i>TP53</i>	NM_000546.5	chr17	7577538	C	T	c.743G>A	p.R248Q	4.28 (273/6383)
21019	<i>TP53</i>	NM_000546.5	chr17	7577106	G	A	c.832C>T	p.P278S	5.56 (440/7903)
21019	<i>TP53</i>	NM_000546.5	chr17	7577120	C	T	c.818G>A	p.R273H	15.34 (1286/8382)
21021	<i>TP53</i>	NM_000546.5	chr17	7577121	G	A	c.817C>T	p.R273C	26.49 (656/2473)
21022	<i>NOTCH1</i>	NM_017617.3	chr9	139390861	G	A	c.7330C>T	p.Q2444*	18.12 (1219/6726)
21045	<i>SF3B1</i>	NM_012433.2	chr2	198266834	T	C	c.2098A>G	p.K700E	11.07 (350/3163)
21046	<i>XPO1</i>	NM_003400.3	chr2	61719471	T	A	c.1712A>T	p.E571V	14.34 (663/4625)
21047	<i>MGA</i>	NM_001164273.1	chr15	42042450	TC	T	c.6646_6646delC	p.Q2216fs*22	29.7 (1549/5215)
21047	<i>SF3B1</i>	NM_012433.2	chr2	198267361	T	C	c.1996A>G	p.K666E	40.33 (1914/4745)
21048	<i>MAP2K1</i>	NM_002755	chr15	66727453	A	G	c.169A>G	p.K57E	13.53 (710/5245)
21048	<i>RPS15</i>	NM_001018.3	chr19	1440423	G	A	c.400G>A	p.G134R	20.62 (632/3064)
21050	<i>ATM</i>	NM_000051.3	chr11	108143456	C	G	c.3161C>G	p.P1054R	46.61 (2718/5829)
21050	<i>NOTCH1</i>	NM_017617.3	chr9	139390765	CG	C	c.7425_7425delC	p.V2475*	19.53 (739/3781)
21050	<i>NOTCH1</i>	NM_017617.3	chr9	139390648	CAG	C	c.7541_7542delCT	p.P2514fs*4	20.79 (794/3815)
21051	<i>SF3B1</i>	NM_012433.2	chr2	198267491	C	A	c.1866G>T	p.E622D	14.5 (744/5129)

21095	<i>SF3B1</i>	NM_012433.2	chr2	198266834	T	C	c.2098A>G	p.K700E	10.71 (596/5558)
21095	<i>TP53</i>	NM_000546.5	chr17	7578375	GCTAT	G	c.551_554delATAG	p.D184fs*62	36.15 (2539/7008)
21098	<i>NOTCH1</i>	NM_017617.3	chr9	139390648	CAG	C	c.7541_7542delCT	p.P2514fs*4	77.44 (3453/4448)
21099	<i>TP53</i>	NM_000546.5	chr17	7578461	C	A	c.469G>T	p.V157F	17.9 (1408/7866)
21189	<i>RPS15</i>	NM_001018.3	chr19	1440414	C	T	c.391C>T	p.P131S	30.92 (983/3178)
21190	<i>NOTCH1</i>	NM_017617.3	chr9	139390648	CAG	C	c.7541_7542delCT	p.P2514fs*4	17.07 (320/1873)
21190	<i>ZMYM3</i>	NM_201599	chrX	70461153	TA	T	c.3807_3807delT	p.I1270fs*2	12.8 (210/1563)
21191	<i>NOTCH1</i>	NM_017617.3	chr9	139390648	CAG	C	c.7541_7542delCT	p.P2514fs*4	22.05 (484/2190)
21193	<i>RPS15</i>	NM_001018.3	chr19	1440436	C	T	c.413C>T	p.S138F	21.18 (270/1275)
21193	<i>TP53</i>	NM_000546.5	chr17	7577570	C	G	c.711G>C	p.M237I	23.01 (421/1829)
21194	<i>TP53</i>	NM_000546.5	chr17	7578460	A	T	c.470T>A	p.V157D	33.24 (995/2990)
21196	<i>EGR2</i>	NM_000399.3	chr10	64573332	C	T	c.1066G>A	p.E356K	46.87 (2378/5070)
21196	<i>NFKBIE</i>	NM_004556.2	chr6	44232738	TGTAA	T	c.759_762delTTAC	p.Y254fs*13	29.99 (702/2340)
21296	<i>NFKBIE</i>	NM_004556.2	chr6	44232738	TGTAA	T	c.759_762delTTAC	p.Y254fs*13	23.85 (899/3770)
21300	<i>NOTCH1</i>	NM_017617.3	chr9	139390648	CAG	C	c.7541_7542delCT	p.P2514fs*4	13.51 (302/2235)
21300	<i>ZMYM3</i>	NM_201599	chrX	70471427	CT	C	c.691_691delA	p.S231fs*26	55.71 (1093/1962)
21301	<i>NOTCH1</i>	NM_017617.3	chr9	139390648	CAG	C	c.7541_7542delCT	p.P2514fs*4	28.54 (764/2673)
21301	<i>SAMHD1</i>	NM_015474	chr20	35526278	C	T	c.1693G>A	p.A565T	52.67 (2193/4164)
21302	<i>ATM</i>	NM_000051.3	chr11	108200961	G	A	c.7328G>A	p.R2443Q	13.56 (480/3539)
21304	<i>IKZF3</i>	NM_012481.4	chr17	37947776	A	C	c.485T>G	p.L162R	14.63 (936/6389)
21304	<i>MGA</i>	NM_001164273.1	chr15	42021500	CA	C	c.3797_3797delA	p.Q1266fs*25	24.72 (1448/5854)
21304	<i>MGA</i>	NM_001164273.1	chr15	41988277	A	AT	c.1069_1070insT	p.A358fs*5	26.82 (1201/4466)
21307	<i>RPS15</i>	NM_001018.3	chr19	1440421	T	G	c.398T>G	p.I133S	39.94 (1203/3010)
21308	<i>SF3B1</i>	NM_012433.2	chr2	198266834	T	C	c.2098A>G	p.K700E	13.08 (289/2206)
23050	<i>BIRC3</i>	NM_001165.4	chr11	102207656	AC	A	c.1639_1639delC	p.Q547fs*21	28.5 (2711/9510)
23050	<i>TP53</i>	NM_000546.5	chr17	7578542	G	C	c.388C>G	p.L130V	41.1 (1803/4386)
23054	<i>ATM</i>	NM_000051.3	chr11	108155201	G	A	c.3993+1G>A	-	30 (1106/3695)
23054	<i>ATM</i>	NM_000051.3	chr11	108143456	C	G	c.3161C>G	p.P1054R	52.2 (2399/4595)
23054	<i>RPS15</i>	NM_001018.3	chr19	1440432	C	T	c.409C>T	p.H137Y	35.4 (955/2699)
23057	<i>ATM</i>	NM_000051.3	chr11	108142006	C	T	c.2950C>T	p.Q984*	94.5 (1768/1870)
23057	<i>XPO1</i>	NM_003400.3	chr2	61719472	C	T	c.1711G>A	p.E571K	53.4 (1504/2814)
23057	<i>ZMYM3</i>	NM_201599	chrX	70469355	G	A	c.1426C>T	p.Q476*	82.8 (3236/3906)
23058	<i>NFKBIE</i>	NM_004556.2	chr6	44232738	TGTAA	T	c.759_762delTTAC	p.Y254fs*13	16.57 (643/3879)
23058	<i>NOTCH1</i>	NM_017617.3	chr9	139390648	CAG	C	c.7541_7542delCT	p.P2514fs*4	40.75 (2095/5133)
23063	<i>ATM</i>	NM_000051.3	chr11	108160350	C	T	c.4258C>T	p.L1420F	47.8 (3023/6316)
23063	<i>SF3B1</i>	NM_012433.2	chr2	198266834	T	C	c.2098A>G	p.K700E	12.2 (786/6441)
23065	<i>MYD88</i>	NM_002468.4	chr3	38182641	T	C	c.794T>C	p.L265P	17.3 (184/1063)
23068	<i>NFKBIE</i>	NM_004556.2	chr6	44232738	TGTAA	T	c.759_762delTTAC	p.Y254fs*13	49.6 (3380/6806)
23070	<i>BIRC3</i>	NM_001165.4	chr11	102207672	C	T	c.1654C>T	p.Q552*	17.82 (784/4399)

23070	NOTCH1	NM_017617.3	chr9	139390648	CAG	C	c.7541_7542delCT	p.P2514fs*4	27.71 (908/3276)
23074	SF3B1	NM_012433.2	chr2	198266611	C	T	c.2225G>A	p.G742D	46.2 (3284/7103)
23075	ATM	NM_000051.3	chr11	108114679	G	A	c.497-1G>A	-	39.35 (1672/4249)
23075	ATM	NM_000051.3	chr11	108172375	T	A	c.5178T>A	p.C1726*	39.99 (2785/6963)
23075	ATM	NM_000051.3	chr11	108160350	C	T	c.4258C>T	p.L1420F	49.89 (3499/7013)
23075	RPS15	NM_001018.3	chr19	1440432	C	T	c.409C>T	p.H137Y	16.41 (462/2814)
23076	XPO1	NM_003400.3	chr2	61719303	C	A	c.1754G>T	p.C585F	48.6 (3396/6977)
23077	ATM	NM_000051.3	chr11	108119720	G	GA	c.1126_1127insA	p.S377fs*2	27.7 (1263/4552)
23077	SF3B1	NM_012433.2	chr2	198266834	T	C	c.2098A>G	p.K700E	49 (3488/7113)
23078	EGR2	NM_000399.3	chr10	64573248	G	T	c.1150C>A	p.H384N	48.7 (3886/7965)
23079	NOTCH1	NM_017617.3	chr9	139390648	CAG	C	c.7541_7542delCT	p.P2514fs*4	10.8 (530/4866)
23079	NRAS	NM_002524.4	chr1	115258744	C	T	c.38G>A	p.G13D	49.2 (1884/3822)
23080	SF3B1	NM_012433.2	chr2	198266494	T	C	c.2342A>G	p.D781G	18.87 (783/4148)
23082	NFKBIE	NM_004556.2	chr6	44232738	TGTAA	T	c.759_762delTTAC	p.Y254fs*13	29.36 (1477/5030)
23082	SAMHD1	NM_015474	chr20	35555633	CAT	C	c.646_647delAT	p.M216fs*2	39.39 (1530/3884)
23082	SF3B1	NM_012433.2	chr2	198266834	T	C	c.2098A>G	p.K700E	35.09 (2582/7357)
23085	SF3B1	NM_012433.2	chr2	198266834	T	C	c.2098A>G	p.K700E	26.24 (415/1581)
23086	FBXW7	NM_033632.3	chr4	153247366	C	T	c.1436G>A	p.R479Q	44.08 (1792/4067)
23086	MGA	NM_001164273.1	chr15	42042600	AG	A	c.6796_6796delG	p.N2267fs*68	72.5 (1002/1382)
23088	SF3B1	NM_012433.2	chr2	198266834	T	C	c.2098A>G	p.K700E	18.17 (714/3929)
23089	NOTCH1	NM_017617.3	chr9	139390145	T	C	c.*378A>G	-	10 (507/5041)
23089	SF3B1	NM_012433.2	chr2	198266834	T	C	c.2098A>G	p.K700E	29.7 (1230/4141)
23091	TP53	NM_000546.5	chr17	7577538	C	T	c.743G>A	p.R248Q	44.2 (2624/5938)
23093	MYD88	NM_002468.4	chr3	38182641	T	C	c.794T>C	p.L265P	50.22 (4631/9220)
23094	ASXL1	NM_015338.5	chr20	31023328	CT	C	c.2814_2814delT	p.A939fs*6	10.3 (750/7309)
23094	ASXL1	NM_015338.5	chr20	31022628	G	T	c.2113G>T	p.E705*	32.6 (2222/6818)
23094	XPO1	NM_003400.3	chr2	61719472	C	T	c.1711G>A	p.E571K	11.6 (794/6847)
23096	NOTCH1	NM_017617.3	chr9	139390648	CAG	C	c.7541_7542delCT	p.P2514fs*4	15.47 (442/2857)
23097	KRAS	NM_033360.2	chr12	25378562	C	T	c.436G>A	p.A146T	14.8 (970/6527)
23106	NOTCH1	NM_017617.3	chr9	139390648	CAG	C	c.7541_7542delCT	p.P2514fs*4	17.4 (611/3508)
23106	POT1	NM_015450.2	chr7	124499045	T	C	c.668A>G	p.Y223C	38.3 (1714/4469)
23106	RPS15	NM_001018.3	chr19	1440417	G	A	c.394G>A	p.G132S	39.1 (1066/2723)
23107	NFKBIE	NM_004556.2	chr6	44232738	TGTAA	T	c.759_762delTTAC	p.Y254fs*13	14.2 (746/5269)
23108	SF3B1	NM_012433.2	chr2	198265476	T	C	c.2681A>G	p.D894G	23.7 (1147/4840)
23112	SF3B1	NM_012433.2	chr2	198266834	T	C	c.2098A>G	p.K700E	38.5 (2460/6375)
23113	TP53	NM_000546.5	chr17	7577551	C	T	c.730G>A	p.G244S	55.6 (1837/3302)
23115	EGR2	NM_000399.3	chr10	64573332	C	T	c.1066G>A	p.E356K	16.35 (1084/6629)
23118	NOTCH1	NM_017617.3	chr9	139390793	CGTGGGCA	C	c.7391_7397delTGCCAC	p.L2464fs*11	29.7 (603/2028)
23118	POT1	NM_015450.2	chr7	124537227	T	A	c.1A>T	p.M1L	23.9 (579/2414)

23118	ZMYM3	NM_201599	chrX	70469448	C	A	c.1333G>T	p.G445*	15 (332/2200)
23118	ZMYM3	NM_201599	chrX	70469002	G	T	c.1488C>A	p.Y496*	49.6 (1038/2089)
23120	NFKBIE	NM_004556.2	chr6	44232738	TGTAA	T	c.759_762delTTAC	p.Y254fs*13	25.22 (915/3627)
23121	NFKBIE	NM_004556.2	chr6	44232738	TGTAA	T	c.759_762delTTAC	p.Y254fs*13	20.3 (645/3175)
23124	IKZF3	NM_183229.2	chr17	37947776	A	C	c.485T>G	p.L162R	14.2 (764/5348)
23127	ATM	NM_000051.3	chr11	108143456	C	G	c.3161C>G	p.P1054R	49.66 (5187/10444)
23128	NFKBIE	NM_004556.2	chr6	44232738	TGTAA	T	c.759_762delTTAC	p.Y254fs*13	19.5 (786/4029)
23129	NOTCH1	NM_017617.3	chr9	139390648	CAG	C	c.7541_7542delCT	p.P2514fs*4	15.34 (393/2561)
23129	SF3B1	NM_012433.2	chr2	198266711	T	C	c.2221A>G	p.K741E	45.5 (3228/7081)
23129	XPO1	NM_003400.3	chr2	61719472	C	T	c.1711G>A	p.E571K	45.4 (4136/9097)
23131	SF3B1	NM_012433.2	chr2	198267491	C	A	c.1866G>T	p.E622D	39 (3585/9180)
23132	MGA	NM_001164273.1	chr15	41961741	C	T	c.649C>T	p.Q217*	29.8 (2153/7211)
23132	XPO1	NM_003400.3	chr2	61719472	C	T	c.1711G>A	p.E571K	38 (2909/7641)
23133	IKZF3	NM_183229.2	chr17	37947776	A	C	c.485T>G	p.L162R	21.04 (1759/8358)
23133	NOTCH1	NM_017617.3	chr9	139390648	CAG	C	c.7541_7542delCT	p.P2514fs*4	11.85 (574/4841)
23133	ZMYM3	NM_201599	chrX	70469358	G	A	c.1423C>T	p.Q475*	21.18 (805/3800)
23135	MYD88	NM_002468.4	chr3	38182259	T	C	c.695T>C	p.M232T	29.1 (1890/6486)
23137	SF3B1	NM_012433.2	chr2	198266611	C	T	c.2225G>A	p.G742D	31.9 (2402/7525)
23140	SF3B1	NM_012433.2	chr2	198267369	G	A	c.1988C>T	p.T663I	39.18 (2933/7485)
23141	IKZF3	NM_183229.2	chr17	37947776	A	C	c.485T>G	p.L162R	44.6 (2695/6031)
23143	SF3B1	NM_012433.2	chr2	198266834	T	C	c.2098A>G	p.K700E	23.88 (1942/8129)
23145	ATM	NM_000051.3	chr11	108155085	A	G	c.3878A>G	p.N1293S	36.6 (2670/7285)
23145	IKZF3	NM_183229.2	chr17	37947776	A	C	c.485T>G	p.L162R	38.14 (2282/5983)

Table S4. 11q deletion, 17p deletion and *TP53* mutational status of tumor cell lines and primary CLL cells

Sample ID	11q deleted	17p deleted	<i>TP53</i> mutated
MEC1	no	yes	no
SSK41	no	no	no
VL51	no	yes	no
JEKO1	no	yes	yes
MAVER1	yes	yes	yes
Z138	no	no	no
9321	no	no	no
14462	yes	no	no
12603	no	no	no
11731	no	no	no
12600	no	no	no

Table S5. Primary cell lines divided into *BIRC3*/*TP53* mutated or wild-type (WT).

Sample ID	<i>IGHV</i>	<i>TP53</i>	<i>BIRC3</i>
13443	Unmutated	WT	Mutated
9696	Unmutated	WT	Mutated
9482	Unmutated	WT	Mutated
14324	Unmutated	WT	Mutated
PMN019	Unmutated	WT	Mutated
PMN012	Unmutated	WT	Mutated
11480	Unmutated	Mutated	WT
13344	Unmutated	Mutated	WT
7916	Unmutated	Mutated	WT
13730	Unmutated	Mutated	WT
9311	Unmutated	Mutated	WT
PMN081	Mutated	Mutated	WT
14326	Unmutated	Mutated	WT
11214	Unmutated	Mutated	WT
10666	Unmutated	WT	WT
11815	Unmutated	WT	WT
19361	Unmutated	WT	WT
10872	Unmutated	WT	WT
10650	Unmutated	WT	WT
PMN059	Unmutated	WT	WT
10320	Unmutated	WT	WT